Visual recognition is heralded by shifts in local field potential oscillations and inhibitory networks in primary visual cortex

Abbreviated title: Experience-dependent oscillations in V1

Dustin J. Hayden[1*], Daniel P. Montgomery[1*], Samuel F. Cooke[2], Mark F. Bear[1]

1 - The Picower Institute for Learning and Memory, Department of Brain and Cognitive Sciences, Massachusetts Institute of Technology, Cambridge, US 02139
2 -The MRC Centre for Neurodevelopmental Disorders, Department of Basic and Clinical Neurosciences, The Institute of Psychiatry, Psychology and Neuroscience, King's College London, London, UK SE5 9RT

* Authors contributed equally to the work

Correspondence:
Mark Bear
Department of Brain and Cognitive Sciences
Massachusetts Institute of Technology
Cambridge, MA, USA 02139
mbear@mit.edu

Number of pages: 26
Abstract: 200 words
Introduction: 407 words
Discussion: 2337 words
Number of figures/tables: 11/0
Number of supplemental figures: 2

The authors declare no competing financial interests.

Abstract:

Filtering out familiar, irrelevant stimuli eases the computational burden on the cerebral cortex. Inhibition is a candidate mechanism in this filtration process. Oscillations in the cortical local field potential (LFP) serve as markers of the engagement of different inhibitory neurons. In awake mice, we find pronounced changes in LFP oscillatory activity present in layer 4 of primary visual cortex (V1) with progressive stimulus familiarity. Over days of repeated stimulus presentation, low frequency (alpha/beta ~15 Hz peak) power increases while high frequency (gamma ~65 Hz peak) power decreases. This high frequency activity re-emerges when a novel stimulus is shown. Thus, high frequency power is a marker of novelty while low frequency power signifies familiarity. Two-photon imaging of neuronal activity reveals that parvalbumin-expressing inhibitory neurons disengage with familiar stimuli and reactivate to novelty, consistent with their known role in gamma oscillations, whereas somatostatin-expressing inhibitory neurons show opposing activity patterns, indicating a contribution to the emergence of lower frequency oscillations. We also reveal that stimulus familiarity and novelty have differential effects on oscillations and cell activity over a shorter timescale of seconds. Taken together with previous findings, we propose a model in which two interneuron circuits compete to drive familiarity or novelty encoding.

Keywords:

learning, memory, plasticity, novelty, interneuron, gamma

Introduction:

The awake brain receives a steady stream of sensory stimuli. Distinguishing novel, potentially relevant stimuli from familiar, irrelevant stimuli is essential for the dedication of energy and attention to only those elements of the environment that may be salient for survival. Previous studies have described an electrophysiological signature of long-term recognition memory within primary visual cortex (V1) of mice that is highly selective for stimulus attributes, such as orientation[1,2]. Over days of repeated presentation of a simple, phase-reversing sinusoidal grating stimulus, the magnitude of visually evoked potentials (VEPs) recorded in layer 4 of V1 in awake, head-fixed mice significantly increases. We refer to this process as stimulus-selective response plasticity (SRP). Similar phenomena have been reported by other laboratories[3-6].

Much headway has been made in understanding the requirements for SRP. Disruption of SRP by treatments local to V1, notably including manipulations of NMDA receptor (NMDAR) function and AMPA receptor trafficking in principal cells, had suggested involvement of the mechanisms of long-term potentiation (LTP) of feedforward excitatory synapses[1,7]. However, more recent studies show that SRP is (1) not supported by plasticity at excitatory layer 4 synapses[8,9] and (2) depends on the activity of parvalbumin-expressing (PV+) neurons in V1[10]. Given the extensive evidence that PV+ inhibitory neurons contribute to gamma oscillations in the cortex[11-18], in the current study we sought to understand how the local field potential (LFP) and PV+ cell activity in layer 4 are influenced by stimulus familiarity and how these changes evolve over time.

We found that exposure of mice to a novel visual stimulus elicits high frequency (~65 Hz) oscillations in the LFP and increases PV+ cell activity measured using two-photon (2-p) calcium imaging. With repeated viewing over days, the now-familiar stimulus elicited reduced high frequency power in the LFP with a corresponding decrease in PV+ cell activity, as well as a sharp increase in low frequency (~15 Hz) oscillations. These observations are consistent with the hypothesis that familiar stimuli recruit a population of somatostatin-expressing (SOM+) interneurons that promote beta oscillations and inhibit PV+ neurons[16,19]. Indeed, 2-p imaging of GCaMP7f expressed in SOM+ revealed a profound increase in their activity during familiar stimulus viewing. These signatures of familiar stimulus recognition did not appear immediately on stimulus onset, but developed rapidly within the first few seconds of visual stimulation. Our findings significantly advance the understanding of how visual recognition memory is expressed at the circuit level and demonstrate how stimulus familiarity imposes oscillatory activity on cerebral cortex.

Materials and Methods:

Mice

All procedures adhered to the guidelines of the National Institutes of Health and were approved by the Committee on Animal Care at MIT, Cambridge, MA, USA. For local field potential experiments, we used male and female mice between P26-70 on a C57BL/6 background (Charles River laboratory international, Wilmington, MA). For calcium imaging experiments, we used male and female PV-Cre mice (B6.129P2-Pvalb$^{tm1(cre)Arbr}$/J, RRID:IMSR JAX:017320) and SOM-Cre mice (B6N.Cg-Sst$^{tm2.1(cre)Zjh}$/J, RRID:IMSR JAX:018973). Animals were housed in groups of 2-5 same-sex littermates after weaning at postnatal day (P) 21. They had access to food and water ad libitum and were maintained on a 12 hour light-dark cycle.

Surgery

Young adult C57BL/6 mice (P26-P52) were first injected with 0.1 mg/kg Buprenex subcutaneously (s.c.) to provide analgesia. Induction of anesthesia was achieved via inhalation of isoflurane (3% in oxygen) and thereafter maintained via inhalant isoflurane (~1-2% in oxygen). Prior to surgical incision, the head was shaved and the scalp cleaned with povidone–iodine (10% w/v) and ethanol (70% v/v). Scalp was resected and the skull surface was scored. A steel headpost (anterior to bregma) was affixed to the skull with cyanoacrylate glue. Small burr holes were drilled above both hemispheres of binocular V1 (3.0 mm lateral of lambda). Tapered 300-500 MΩ tungsten recording electrodes (FHC, Bowdoin, ME, US), 75 µm in diameter at their widest point were implanted in each hemisphere, 450 µm below cortical surface. Silver wire (A-M systems, Sequim, WA, US) reference electrodes were placed within cingulate cortex. Electrodes were secured using cyanoacrylate and the skull was covered with dental cement. Nonsteroidal anti-inflammatory drugs were administered upon return to the home cage (meloxicam, 1 mg/kg s.c.). Signs of infection and discomfort were carefully monitored. Mice were allowed to recover for at least 48 hours prior to head-fixation.

For cranial window implantations for two-photon calcium imaging, adult PV-Cre or SOM-Cre mice (P50-P70) were anesthetized and prepared as described above. Following scalp incision, a lidocaine (1%) solution was applied onto the periosteum and the exposed area of skull gently scraped with a scalpel blade. Then, a 3 mm craniotomy was made over binocular V1. Adeno-associated virus containing the GCaMP7f gene (pGP-AAV9-syn-FLEX-jGCaMP7f-WPRE, 104488-AAV9, Addgene, Watertown, MA, USA) was loaded into a glass micropipette with a tip diameter of 40–50 µm attached to a Nanoject II injection system (Drummond Scientific, Broomall, PA, USA). The micropipette was then inserted into binocular V1 layer 4 at depths of 400 and 450 µm below pial surface and ~50 nl virus was delivered at each depth. Next, a sterile 3 mm round glass coverslip (CS-3R-0, Warner Instruments, Hamden, CT, USA) was gently laid on top of the exposed dura mater. The coverslip was secured with cyanoacrylate glue and a stainless steel head post was attached to the skull. Once the glue had set, dental acrylic (C&B Metabond Quick Adhesive Cement System, Parkell, NY, USA) was mixed and applied throughout the exposed skull surface.

Stimulus delivery

Prior to stimulus delivery, mice were acclimated to the restraint in front of a gray screen for a 30-minute session on each of two consecutive days. On stimulus presentation days, mice were presented with 5 blocks of 100 phase-reversals of each oriented stimulus. Each stimulus block was preceded by a period of gray screen, a period of black screen, and another period of gray screen. Gray periods lasted 6 or 12 s and black periods lasted 10 or 20 s, depending on the recording system. Discrete sections of gray and black screen viewing were timestamped for later normalization. Visual stimuli consisted of full-field, 100% contrast, sinusoidal gratings that were presented on a computer monitor. Visual stimuli were generated using custom software written in either C++ for interaction with a VSG2/2 card (Cambridge Research systems, Kent, U.K.) or Matlab (MathWorks, Natick, MA, U.S.) using the PsychToolbox extension (http://psychtoolbox.org) to control stimulus drawing and timing. These full-field sinusoidal grating stimuli phase-reversed at a frequency of 0.5 Hz. Grating stimuli spanned the full range of monitor display values between black and white, with gamma-correction to ensure constant total luminance in both gray-screen and patterned stimulus conditions. Throughout, stimulus orientation varied such that a novel orientation was always a minimum of 25° different from any experienced previously by the individual mouse and was never within 20° of horizontal because

these orientations are known to elicit visually-evoked potentials of greater magnitude than vertical or oblique stimuli. If more than 1 orientation was shown within a session, stimuli were pseudo-randomly interleaved such that 3 consecutive presentations of the same stimulus never occurred.

In vivo electrophysiology experimental design and analysis

Electrical recordings were conducted in awake, head-restrained mice. Recordings were amplified and digitized using the Recorder-64 system (Plexon Inc., Dallas, TX, US) or the RHD Recording system (Intan Technologies, Los Angeles, CA, US). Two recording channels were dedicated to recording continuous local field potential from V1 in each implanted hemisphere. In a subset of experiments, an additional third recording channel was reserved for the Piezo-electrical input carrying the forepaw movement. Local field potential was recorded from V1 with 1 kHz sampling. On the Plexon system, we used a 500 Hz low-pass filter. On the Intan system, we used a 0.1 Hz high pass and a 7.5 kHz low pass filter. Local field potential data and piezo-electric data was imported (see Importing and data cleaning) and the local field potential's spectral content was analyzed (see Spectral analysis). In a subset of experiments, forepaw movement was analyzed (see Movement analysis). In a separate experiment, pupil dilation was monitored (see Pupil analysis).

In vivo two-photon calcium imaging

Three to four weeks following craniotomy surgery, the mice were habituated to the behavior restraint apparatus in front of a gray screen with the objective lens of the two-photon microscope positioned on the head plate for 30 min for two consecutive days. A Ti:sapphire laser (Coherent, Santa Clara, CA, USA) was used for imaging at a wavelength of 930 nm. Photomultiplier tubes (Hamamatsu, Japan) and the objective lens (20×, 0.95 NA, XLUMPLFLN, Olympus, Japan) were used to detect fluorescence images. Calcium image recordings were triggered by time-locked TTL pulses generated from USB-1208fs (Measurement Computing, Norton, MA, USA) using the Prairie view and TriggerSync Software (Bruker, CA, USA) and imaged at a frequency of ~2.8 Hz at the depth of ~350 μm in V1. The size of the imaging field of view was ~600 x 600 μm^2 at 256 x 256 pixels.

Pupillometry

To track the pupil during head fixation, we used a Blackfly S USB3 camera (FLIR Systems, Inc., Wilsonville, OR, US) with a 1.0X lens (Edmund Optics, Inc., Barrington, NJ, US). The left eye was illuminated with a 780 nm infrared LED light source (Thorlabs, Inc., Newton, NJ, US). A small tissue was placed over the light source. Images were acquired at 20 frames per second during stimulus presentation and each frame emitted a voltage signal into the RHD Recording system for later alignment with stimulus presentations. A subset of videos were used for training the top and bottom edge of the pupil on DeepLabCut[20]. All videos were evaluated with the trained network. The output of DeepLabCut includes the x,y-coordinate of the top and bottom edge as well as the certainty of the location. Both were used in our analysis (see Import and data cleaning and Pupil analysis).

Importing and data cleaning

All analyses were conducted using custom MATLAB code and the Chronux toolbox[21]. All code is available upon reasonable request. Briefly, the local field potential from each

channel was extracted and converted to microvolts. Data was then zero-meaned and de-trended using a 1 second sliding window and a 500 ms step size. A 3rd-order Butterworth filter was used to notch frequencies between 58 and 62 Hz. Piezo-electric data was zero-meaned and rectified. Pupil edges that had less than 100% certainty of location in terms of DeepLabCut output (see Pupillometry) were ignored and a spline interpolation was used to recover the missing points. Qualitatively, these periods of uncertain pupil edge location occurred frequently during black screen and rarely during gray screen or stimulus presentation.

Spectral analysis

Given that the visually-evoked potential violates assumptions required for spectral analysis (namely second-order stationarity), we only analyzed the spectral activity between 400 ms and 2000 ms after a phase-reversal. We computed the multi-tapered spectrogram of the local field potential using the Chronux toolbox[21]. The parameters used were: a 500 ms sliding window, a 100 ms step size, zero-padded to the 2nd power, and 5 tapers with a time-bandwidth product of 3. We also computed the multi-tapered spectrum using the same parameters, but including all data between 400 ms and 2000 ms. To calculate the normalized spectrum/spectrogram, we found the median spectrum/spectrogram of the animal's black screen and took 10*log10(stimulus_spectrum/median_black_spectrum). This is reported as a decibel (dB).

Concatenated spectrum analysis

Given the contamination by the visually-evoked potential, we concatenated the normalized spectrums. This concatenated spectrum utilizes the multi-tapered spectrum of the period between 400 and 2000 ms after a phase-reversal. Ordering these spectrums by their presentation number and representing power as a color generated the concatenated spectrum. For each presentation, we calculated the max power within the 10-30 Hz frequency band as well as the 60-80 Hz frequency band. By visual inspection, it seemed like no changes were seen in the concatenated spectrum after 25 presentations, so we used the average of the max power for presentations 26-100 as a metric to compare the first few presentations to in our bootstrapping procedure. Given that no significant difference is found between presentations after the 15th and the average of presentations 26-100, we can be reasonably certain or split was logical. Other splits were tried and there were no qualitative differences in the resulting data.

Block onset spectral analysis

For this analysis, we only used the group of animals that had 6 second gray periods and 10 second black periods (see Stimulus delivery). The local field potential data within 12 seconds of block onset (both before and after) was extracted and separated into overlapping 400 ms chunks each with centers spaced 100 ms apart. For each chunk, we computed the normalized spectrum (see Spectral analysis). Transitions from black to gray, gray to stimulus, and between phase 0° and phase 180° will elicit a visually-evoked potential. Thus, for each frequency within the normalized spectrum, we removed contaminated regions and interpolated between them using cubic interpolation. Specifically, we removed the chunks whose midpoints were between 100 ms before and 500 ms after a transition. The trailing edge (near 12 seconds) was not included due to the edge artifacts of interpolation. Once we had the interpolated normalized spectrum, we found the max power in the 10-30 Hz frequency band and the 60-80 Hz frequency band for each chunk.

P-Episode analysis

P-Episode is a method that quantifies the fraction of time that oscillations exceed amplitude and duration thresholds[22,23]. We lightly adapted analysis software kindly provided by Marieke van Vugt. Briefly, Mortlet wavelets between 7 and 100 Hz with a wavenumber of 5 were used to extract spectral information from both black and stimulus periods. Then, to obtain an estimate of pink noise, we fit the black spectrum with a linear regression in log-log space and stored the mean power values at each frequency (using the trained regression parameters). This was done for each black period and ultimately averaged to get one estimate of pink noise per animal. In line with default parameters, the power threshold was determined for each frequency as the 95th percentile of the chi-squared probability distribution with 2 degrees of freedom. The duration threshold was simply three cycles. Next, for each presentation of a stimulus, the above Mortlet wavelets were used to extract spectral information. Finally, for each time point, it was determined whether a given frequency exceeded both the power and duration threshold. If it exceeded both thresholds, the time point was in that oscillation. Otherwise, the time point was not in that oscillation. Herein we report the percent of time in an oscillation for each of the analyzed frequencies.

Correlations

We analyzed the correlation of VEP magnitude and LFP power. Because the VEP in response to each phase reversal is variable and can be obscured by ongoing voltage fluctuations, it had to exceed a threshold to be included in the analysis. For each animal, we computed the average activity during exposure to gray screen between each block of stimuli. The gray period was sampled at the same frequency and duration as used for VEP analysis. The difference between the minimum of this average gray activity (within 100 ms of the sample onset) and the maximum of this average gray activity (any time after the minimum) was taken as our voltage threshold. Next, we computed the average VEP above threshold for all familiar and novel presentations to get the indices for the positive and negative peaks (regardless of stimulus). Then, for each phase-reversal, we calculated the magnitude of the difference between the positive and negative peak. If this VEP magnitude was below the voltage threshold decided by the gray screen period, it was discounted. We also eliminated the first presentation of each block considering we were comparing the pre-phase-reversal LFP to the VEP magnitude and the first presentation's LFP would be during gray screen. The average voltage of the first ten ms after a phase-reversal was subtracted from each individual trace to align them.

For each phase-reversal, we also calculated the normalized spectrum for the 400 ms leading into the phase-reversal. Using this, we obtained the max power within the 10-30 Hz frequency band and the 60-80 Hz frequency band. For correlation analysis, we used a simple Pearson correlation coefficient. Correlation analysis could be done on just familiar data, just novel data, or an equal random sampling of both. For the purposes of reporting, we selected a single exemplar animal that was most like all reported population median correlations.

Calcium imaging analysis

Acquired time series of calcium imaging files were processed using Suite2p[24]. All recorded files were registered to stabilize shifts due to animal movement. We manually selected regions of interest (ROIs) base on the maximum projection of all frames. We then extracted the fluorescence of each ROI for all time points. For each ROI, we calculated the corrected

fluorescence, which is the raw fluorescence minus 7/10ths of the neuropil's fluorescence[25]. We used the average inter-block gray period to compute the response relative to gray ($F_{stim} - F_{avg_gray}$)/F_{avg_gray}. For our non-parametric bootstrapping procedure, we randomly selected with replacement from the mice we recorded from, randomly selected with replacement from the cells they had, and randomly selected with replacement from said cell's data. This procedure was repeated as outlined in **Statistics**. Only cells that could be tracked over all days were included in our analysis.

Movement analysis

For each stimulus phase-reversal, we smoothed imported piezo-electric data with a moving average over 200 ms. We similarly smoothed periods of gray screen (see Stimulus delivery). We subtracted the median gray screen forepaw movement from the stimulus forepaw movement and report this as normalized movement in arbitrary units (a.u.).

Pupil analysis

The DeepLabCut predicted x,y-coordinates of the top and bottom of the pupil were cleaned (see Importing and data cleaning). Then, the Euclidian distance between the top and bottom of the pupil was calculated to obtain the pupil dilation in pixels.

Statistics

Most statistics were done with the non-parametric hierarchical bootstrap for multi-level data[26]. Briefly, statistical comparisons were between two groups (with each animal belong to both groups due to our within animal experimental design). To begin the bootstrap process, mice were randomly selected with replacement from the population. For each randomly selected mouse, a number of random phase-reversals were selected with replacement from the mouse's group A data. Another random set of phase-reversals were selected with replacement from the mouse's group B data. This data was stored and the process was repeated for each randomly selected animal. Once all data was randomly selected, the mean difference between the randomly selected samples of group A and group B was computed and stored. This entire bootstrap process was repeated 1000 times. Once all 1000 bootstraps had completed, the bootstrapped differences were sorted from lowest to highest value. The 500th value was the median group difference, the 5th value was the lower bound of the 99% confidence interval, and the 995th value was the upper bound of the 99% confidence interval. If the 99% confidence interval does not include zero, we report a statistically significant difference between group A and group B with a small marker below the corresponding data on the plot. To facilitate communication in the results section, we report the identity, median, and 99% confidence interval for the peak significant median difference above and below 50 Hz, if it exists. In most figures, the colored plots are mean +/- SEM of all animals and the gray plots to the right are the 99% bootstrapped confidence interval for those two groups. The only other statistical procedure was a two-sample Kolmogorov-Smirnov test on the data comprising the cumulative distribution functions in **Figure 5**. All data, code, and values are available for complete replication of the paper upon reasonable request.

Results:

Layer 4 local field potential oscillations display variable frequency composition in V1 of awake, head-fixed mice

We acquired local field potential (LFP) data from electrodes chronically implanted within layer 4 of binocular V1 of C57BL6/J mice. Awake, head-fixed mice viewed full field, 0.5 Hz phase-reversing sinusoidal grating stimuli separated into blocks of 100 phase-reversals preceded by periods of gray and black screen (**Figure 1A, B, C**). We used equally-spaced timestamps to segment gray and black data into 2000 ms portions for further normalization and comparison. Under these conditions, we could average the stimulus-evoked LFP waveform occurring within a 400-ms time window from the start of each phase-reversal. This average visually-evoked potential (VEP) is the signal typically used to monitor the emergence of SRP[1,2,7,10]. However, the continuous LFP signal reveals periodic changes from low amplitude, high frequency activity to high amplitude, low frequency activity (**Figure 1D**). Because the portion of the recording containing the VEP violates second-order stationarity, a requirement for oscillatory analysis, we focused our analysis on the last 1600 ms of each 2000 ms presentation (**Figure 1D**). This approach is consistent with previous work[27,28]. The raw spectrogram for each phase-reversal shows that some time periods have strong low frequency oscillations whereas others have strong high frequency oscillations (**Figure 1E**). We chose not to normalize the raw signal to data from a gray screen period because isoluminant gray screens elicit oscillations in the gamma range that emerge in the cortex but arise from a subcortical source[29]. Instead, we normalized the raw spectrogram to the median spectrogram generated during black screen presentation (**Supplementary Figure 1**). The normalized spectrogram again shows phase-reversals with periods of strong low frequency oscillations in the alpha/beta range (10-30 Hz) and periods of high frequency oscillations in the gamma range (60-80 Hz) (**Figure 1F**). The normalized spectral data will be used throughout the remainder of this study.

V1 oscillations are influenced by stimulus familiarity over days

We investigated whether the frequency composition of the V1 LFP in layer 4 changes as a result of visual experience. We induced SRP by exposing mice to a phase-reversing stimulus at a single orientation each day for 6 consecutive days. On day 1, the normalized spectrum displayed strong high frequency power (**Figure 2A**). As the stimuli became familiar over subsequent days, high frequency power diminished and low frequency power increased. Comparing day 6 to day 1 showed day 6 had significantly more low frequency power (**Figure 2B**, *peak: 15.50 Hz, median difference: 2.88 dB, 99% CI = [1.99 3.67] dB, n = 13*) and less high frequency power (**Figure 2B**, *peak: 64.82 Hz, median difference: -1.90 dB, 99% CI = [-3.17 -0.53] dB, n = 13)*. Thus, stimulus familiarity increases low frequency power and decreases high frequency power in layer 4 of V1.

The change in average spectrum power could be a result of a blanket increase in any given frequency at all times, more periods of sustained oscillatory activity, or some combination of both. We therefore measured the amount of time spent by the LFP within each frequency on each day. For our purposes, this was achieved with P-Episode (see Methods), a technique that only counts an oscillation as active if it surpasses both a power and duration threshold[22,23]. On day 1, the LFP spent more time exhibiting high frequency oscillations than low (**Figure 2C**). By day 6, time spent in high frequency oscillations dropped and time spent in low frequency oscillations increased. Comparing day 6 to day 1 revealed that more time was spent in low frequency oscillations on day 6 than day 1 (**Figure 2D**, *peak: 15.00 Hz, median difference: 15.24%, 99% CI = [10.81 20.39]%, n = 13*) and less time was spent in high frequency oscillations on day 6 than day 1 (**Figure 2D**, *peak: 65.00 Hz, median difference: -9.64%, 99% CI*

= [-16.42 -3.61]%, n = 13). Thus, experience with a stimulus increases time spent in low frequency oscillations and decreases time spent in high frequency oscillations.

Experience-dependent oscillations in V1 are stimulus-specific

We next sought to determine if, like SRP, the shift in frequency composition of the LFP was stimulus specific. On day 7, in addition to the now highly familiar stimulus orientation, we presented a novel stimulus that was offset by 90° from familiar. Five blocks of each stimulus were pseudo-randomly interleaved with each other. Consistent with our observation of changes in frequency composition with growing familiarity (**Figure 2**), the familiar stimulus generated more low frequency power and less high frequency power in the layer 4 LFP than the novel stimulus (**Figure 3A**). Bootstrapping confirmed that the familiar orientation produced more low frequency power (**Figure 3B**, *peak: 14.65 Hz, median difference: 3.72 dB, 99% CI = [2.99 4.53] dB, n = 13*) and less high frequency power than the novel orientation (**Figure 3B**, *peak: 67.63 Hz, median difference: -1.92 dB, 99% CI = [-2.80 -1.14] dB, n = 13*). We observed similar results for the time spent in high and low frequency oscillations (**Figure 3C**), with more time spent in low frequency oscillations for the familiar orientation compared to the novel orientation (**Figure 3D**, *peak: 15.00 Hz, median difference: 16.25%, 99% CI = [11.76 21.12]%, n = 13*) and less time spent in high frequency oscillations (**Figure 3D**, *peak: 69.00 Hz, median difference: -11.83%, 99% CI = [-18.88 -6.32]%, n = 13*). Thus, oscillations within V1 are experience-dependent and stimulus-specific.

Neither movement nor arousal account for the changes in layer 4 LFP frequency composition

Studies have shown that locomotion can have a substantial effect on V1 oscillations and response properties in awake mice[30-34]. Given the evidence that SRP and learned suppression of behavior both occur in tandem and require the same mechansisms[7,10], we were interested to understand if oscillations that emerged in V1 LFP with growing familiarity were simply the result of reduced movement. Our previous analysis of behavior during SRP was restricted to the first five seconds after a transition from gray screen to the stimulus, measuring an orienting or startle response that was more likely for novel than familiar stimuli[7]. The oscillations under investigation here extend throughout each stimulus block, over 100 seconds, so it was critical to also analyze the animal's movement throughout. To this end, we recorded piezo-electric activity that measured ongoing forepaw movement (**Figure 4A**). Analysis of the forepaw movement, normalized to gray screen (see Methods), revealed no difference between familiar and novel stimuli when looking throughout all phase-reversals (**Figure 4B**). This was confirmed with non-parametric hierarchical bootstrapping (**Figure 4C**, *the confidence interval included 0*). Thus, the changes in spectral activity driven by stimulus novelty cannot simply be accounted for by movement.

While movement itself may not account for the V1 oscillations that we have reported, changes in the LFP frequency composition could reflect global arousal shifts. Global arousal can be reliably monitored using pupillometry[33,35]. Thus, we tracked pupil dilation as mice underwent the SRP paradigm (**Figure 4D**). Pupil size showed no observable or statistical difference between familiar and novel stimuli (**Figure 4E-F**, *the confidence interval included 0*). Thus, the familiarity-dependent changes in spectral activity that we have described cannot simply be accounted for by a global arousal shift.

Oscillations and VEP magnitudes correlate

Given our previous measurements of increased VEP magnitude during SRP[1,2,7] and the concomitant changes in oscillations described here, we investigated the correlation between these two measures of experience-dependent plasticity. We analyzed the VEP magnitudes elicited by each phase reversal and the LFPs that immediately preceded them (see Methods). Changing the analysis window to the LFP after the VEP did not qualitatively change the results (*data not shown*). Cumulative distribution functions of all valid trials from all mice (see Methods) are shown for the max low frequency (10-30 Hz) power, the max high frequency (60-80 Hz) power, and the VEP magnitude (**Figure 5A-C**). They show that familiar stimulus presentations have more low frequency power (**Figure 5A**, *two-sample Kolmogorov-Smirnov test, $p < 0.01$*), less high frequency power (**Figure 5B**, *two-sample Kolmogorov-Smirnov test, $p < 0.01$*), and larger VEP magnitudes (**Figure 5C**, *two-sample Kolmogorov-Smirnov test, $p < 0.01$*) compared to novel stimulus presentations.

We then proceeded to correlate every combination of the three groups with each other. In **Figure 5 (D, F, H)** we show a representative animal whose dataset is most similar to the population average (all animals shown in **Supplementary Figure 2**). In the exemplar, the max low frequency power negatively correlates with max high frequency power (**Figure 5D**). The population average for all animals shows a ~40% negative correlation regardless of stimulus (**Figure 5E,** *median correlation for both: -0.41, 99% CI = [-0.51 -0.30]; median correlation for familiar: -0.35, 99% CI = [-0.43 -0.25]; median correlation for novel: -0.35, 99% CI = [-0.48 -0.20]; n = 13*). There is no statistical difference between the correlation for familiar and novel stimuli (*median correlation difference: 0.00, 99% CI = [-0.14 0.15], n = 13, data not shown*). In the exemplar, the max low frequency power positively correlates with VEP magnitude (**Figure 5F**). The population shows a ~15-30% correlation depending on stimulus (**Figure 5G,** *median correlation for both: 0.33, 99% CI = [0.25 0.39]; median correlation for familiar: 0.14, 99% CI = [0.08 0.21]; median correlation for novel: 0.24, 99% CI = [0.12 0.33]; n = 13*). However, there is no statistical difference between the correlation for familiar and novel stimuli (*median correlation difference: -0.10, 99% CI = [-0.21 0.03], n = 13, data not shown*). Finally, in the exemplar, the max high frequency power negatively correlates with VEP magnitude (**Figure 5H**). The population shows a ~20% negative correlation regardless of stimulus (**Figure 5I,** *median correlation for both: -0.25, 99% CI = [-0.33 -0.16]; median correlation for familiar: -0.17, 99% CI = [-0.25 -0.09]; median correlation for novel: -0.21, 99% CI = [-0.30 -0.11]; n = 13*). There is no statistical difference between the correlation for familiar and novel stimuli (*median correlation difference: 0.04, 99% CI = [-0.08 0.15], n = 13, data not shown*). Thus, VEPs and low-frequency oscillatory power correlate regardless of stimulus novelty, and both grow with increased familiarity. These data are compatible with the hypothesis that the same underlying biology is responsible for both manifestations of SRP.

Experience-dependent oscillations in V1 emerge over presentations

VEPs and principal cell calcium transients elicited in layer 4 by the transition from gray screen to an oriented grating stimulus are the same for both familiar and novel stimulil[36]. The robust familiar-novel differences observed in time-averaged VEPs and cellular responses emerge during the course of a block of stimulation. We were therefore interested in comparing the LFP oscillations proximal to the first and last phase transition (to phase 0°, called a flip) for each stimulus. Consistent with other measures of SRP, the first flip in a familiar block produced little low frequency power but large high frequency power, whereas the last flip displayed the

expected increase in low frequency power and decrease in high frequency power (**Figure 6A**). Compared to the first flip, the last flip in familiar blocks had more low frequency power (**Figure 6B**, *peak: 21.48 Hz, median difference: 3.16 dB, 99% CI = [1.35 4.92] dB, n = 13*) and less high frequency power (**Figure 6B**, *peak: 67.02 Hz, median difference: -2.72 dB, 99% CI = [-4.49 -0.76] dB, n = 13*). The change in high frequency power, but not low frequency power, was also seen for novel blocks (**Figure 6C**). Compared to the first flip, the last flip in novel blocks had roughly the same low frequency power (**Figure 6D**, *peak: 47.97 Hz, median difference: -1.80 dB, 99% CI = [-3.22 -0.35] dB, n = 13*) and less high frequency power (**Figure 6D**, *peak: 68.73 Hz, median difference: -3.01 dB, 99% CI = [-4.92 -1.33] dB, n = 13*). Thus, prolonged exposure to a stimulus decreases high frequency power regardless of stimulus familiarity, while only familiar stimuli show an increase in low frequency power within a stimulus block.

We were next interested to understand how quickly these dominant modes of background cortical activity emerge. At stimulus onset, the max normalized spectral power in the 10-30 Hz band quickly increased for familiar stimuli (**Figure 6E)**. Unexpectedly, power in this band also increased following novel stimulus onset, but the magnitude of the increase was less than for a familiar stimulus (**Figure 6F**). The max normalized spectral power in the 60-80 Hz band increased abruptly at the transition from black screen to gray screen, as expected [29], and increased further upon exposure to a novel stimulus (**Figure 6G**). Power in this band decreased progressively over the first few phase reversals for both novel and familiar stimuli, but the familiar-novel difference was maintained (**Figure 6H**).

To better understand how oscillations in low and high frequency bands change over the entire course of a recording session, we assessed how the spectral power evolves during a block of visual stimulation. First, we created a concatenated spectrum (**Figure 7A**). Briefly, this concatenated spectrum is composed of the power spectrum for each phase-reversal, excluding the time period containing the VEP (see Methods). In agreement with previous results (**Figure 6**), the first few phase-reversals showed a different oscillatory signature than the last few phase-reversals. The concatenated spectrum appeared to be stable by the 25th phase-reversal (50 sec. from stimulus onset). Thus, for each phase-reversal, we extracted the max power in the 10-30 Hz and 60-80 Hz frequency bands. We used the average of this extracted max power for presentations 26-100 as a comparator in our bootstrapping. For familiar stimuli, regardless of low or high frequency, only the first few phase-reversals displayed a difference from the average of the last phase-reversals (**Figure 7B-E**). Bootstrapping confirmed that only the first presentation shows differences in the low frequency band (**Figure 7C**, *first presentation, median difference: -2.54 dB, 99% CI = [-3.71 -1.10] dB, n = 13*) and in the high frequency band (**Figure 7E**, *first presentation, median difference: 2.03 dB, 99% CI = [0.95 3.03] dB, n = 13*). For novel stimuli, there were interesting dynamics with respect to each frequency band (**Figure 7F-I**). Much like familiar stimuli, max power in the 60-80 Hz band started high and decreased over the first few phase-reversals to reach the steady state level (**Figure 7H-I**, *first presentation, median difference: 2.16 dB, 99% CI = [0.89 3.37] dB, n = 13*). Surprisingly, max power in the 10-30 Hz band started at the average level, increased to a maximum, then decayed back to average (**Figure 7F-G**, *fifth presentation, median difference: 1.95 dB, 99% CI = [0.76 3.11] dB, n = 13*). Thus, oscillations within V1 develop over phase-reversals with experience-dependent changes apparent in the dynamics. These measures suggest that recognition of a familiar stimulus occurs very rapidly, over a few hundred ms. Novel stimuli, in contrast, elicit activity in V1 that can take tens of seconds to reach a steady state.

Experience-dependent oscillations in V1 change between phase-reversals

We next investigated the impact of stimulus familiarity on oscillatory dynamics between phase reversals from the 25th stimulus onward, when it appears that the LFP has reached a steady state. We expected that the spectrogram would show little consistent change over this brief time interval between stimuli. Surprisingly, however, the mean familiar and novel spectrogram showed a consistent time-dependent modulation (**Figure 8A**). To facilitate analysis, we evenly split the spectrogram into early and late components and took the average of each portion. The later portion of a familiar stimulus presentation showed increased low frequency power (**Figure 8A, left**). Compared to the early portion, the late portion of familiar presentations had more low frequency power (**Figure 8B**, *peak: 14.16 Hz, median difference: 0.71 dB, 99% CI = [0.32 1.17] dB, n = 13*). Conversely, the late portion of a novel presentation showed no change in low frequency power but did reveal decreased high frequency power (**Figure 8A, right**). Compared to the early portion, the late portion of novel stimulus presentations had reduced high frequency power (**Figure 8C**, *peak: 71.78 Hz, median difference: -0.61 dB, 99% CI = [-1.05 -0.24] dB, n = 13*). Thus, as an upcoming familiar phase-reversal approaches, low frequency oscillations display an anticipatory strengthening. Conversely, each phase reversal of a novel stimulus is followed by a temporary boost of high frequency oscillations that gradually wane.

Layer 4 PV+ interneuron activity is suppressed as stimuli become familiar

Considerable evidence indicates that PV+ inhibitory neurons play a critical role in the generation of cortical gamma oscillations[11-18]. Given our observation here that novel stimuli elicit high frequency oscillations, our previous work demonstrating that SRP depends on unfettered PV+ cell activity[10], and additional evidence that PV+ cells in layer 2/3 of sensory cortex decrease their activity after repeated passive exposure to a stimulus[19,37], we performed experiments to measure the activity of layer 4 PV+ neurons over days during induction of SRP. We expressed GCaMP7 in PV+ cortical neurons using a Cre-dependent conditional expression system and imaged cells with a 2-p microscope (**Figure 9A**). Only those cells that could be tracked across all days were included in the analysis. The average PV+ cell activity decreased over days as the animal became familiar with the stimulus (**Figure 9B**). Day 4 activity was significantly lower than day 1 activity (**Figure 9C,** *median difference: -0.13 dF/F, 99% CI = [-0.22 -0.04] dF/F, n = 9*). On day 5, when both familiar and novel stimuli were presented, the average PV+ cell activity for each mouse showed a clear increase in activity during novel stimuli compared to familiar stimuli (**Figure 9D**). Non-parametric hierarchical bootstrapping confirmed that familiar stimuli elicited less activity than novel stimuli (**Figure 9E,** *median difference: -0.14 dF/F, 99% CI = [-0.18 -0.10] dF/F, n = 9*). Thus, layer 4 PV+ cells in V1 are activated by novel stimuli and suppressed by familiar stimuli.

Layer 4 SOM+ interneuron activity grows as stimuli become familiar

There is evidence that SOM+ inhibitory neurons contribute to beta oscillations and become more active with experience[19,37-40]. Thus, we also measured the activity of layer 4 SOM+ neurons over days as SRP was induced. As for the PV+ cells, we expressed GCaMP7 in SOM+ cortical neurons using a Cre-dependent conditional expression system and only analyzed cells that could be tracked across all days. The average SOM+ cell activity increased over days (**Figure 9F**). Day 4 activity was significantly higher than day 1 activity (**Figure 9G,** *median difference: 0.22 dF/F, 99% CI = [0.07 0.38] dF/F, n = 7*). On day 5, SOM+ cells were active during familiar stimuli but inactive when viewing novel stimuli (**Figure 9H**). Bootstrapping

confirms that familiar stimuli induced more activity than novel stimuli (**Figure 9I,** *median difference: 0.41 dF/F, 99% CI = [0.28 0.56] dF/F, n = 7*). Thus, layer 4 SOM+ cells in V1 are activated by familiar stimuli and are agnostic during novel stimulus viewing (maintaining gray screen activity levels).

Differences in the activity of PV+ and SOM+ cells during familiar and novel stimulus viewing were extremely robust and surprisingly uniform. In **Figure 10** we compare activity for each neuron on days 1 and 4 as an initially novel stimulus becomes familiar, and the activity to this now-familiar stimulus to a novel orientation (**Figure 10A-B**, n = 1,251 PV+ neurons from 9 mice; **Figure 10C-D**, n = 1,021 SOM+ neurons from 7 mice). As this analysis shows, with very few exceptions, activity of PV+ cells is higher to a novel stimulus than to a familiar stimulus. Conversely, virtually the entire network of SOM+ neurons in layer 4 is more active when a familiar stimulus is viewed than when a novel stimulus is presented.

Discussion:

Originally described in 2006 by Frenkel, Sawtell, et al.[1], SRP is an extremely robust and reliable form of cortical plasticity. As it can be studied under highly constrained experimental conditions using a wide variety of invasive and interventional approaches, it provides a powerful experimental system to understand how the neocortex learns to recognize familiar innocuous stimuli and detect potentially significant novel stimuli[41,42]. A considerable body of prior evidence had suggested that *induction* of SRP requires mechanisms that are shared with the phenomenon of LTP at excitatory synapses on excitatory neurons[1-3,7,8]. Here we used analysis of LFPs and 2-p imaging to examine the hypothesis that *expression* of SRP depends on the differential recruitment of inhibitory networks by familiar and novel visual stimuli. The results show that novel stimuli activate a large population of PV+ interneurons, and that this is manifested, in part, by a substantial increase in the power of high frequency (gamma) oscillations in the layer 4 LFP. As a stimulus becomes familiar, PV+ cell activity and high-frequency oscillations subside, while SOM+ cell activity and low-frequency oscillations sharply increase. Like other manifestations of SRP, these changes in LFP oscillations and interneuron activity are not subtle—they reflect dramatic shifts in the mode of visual information processing as a visual stimulus becomes familiar over days. Although stimulus recognition is not expressed immediately on the transition from a gray screen to a familiar stimulus[36], it does emerge quickly as evidenced by the rapid increase in low-frequency LFP power. Together, these observations constrain the potential mechanisms that give rise to SRP and visual recognition memory.

Differential recruitment of mutually interacting networks of inhibitory neurons herald novelty detection and familiarity recognition

First exposure of a mouse to a novel, unexpected visual stimulus triggers a very rapid increase in high frequency LFP activity in layer 4 of V1, consistent with the strong activation of a large population of PV+ neurons[11-18]. The increase in high frequency oscillations continues during the entire block of stimulation, but does show some relaxation over the course of a few seconds toward a steady-state value. Interestingly however, even during this steady-state period, each phase reversal of the novel stimulus elicits a pulsatile increase in high frequency activity, again suggesting strong feed-forward activation of PV+ interneurons in layer 4. This is the dominant processing mode for novel visual stimuli in V1 of awake mice (**Figure 11**).

One day later, when the stimulus is no longer novel, the PV+ neurons cease to respond strongly during visual stimulation. By the 4th day, presentation of the now-familiar stimulus

instead causes suppression of a substantial fraction of PV+ neurons in layer 4 and, unsurprisingly, there is a clear decrease in the power and duration of high frequency oscillations of the LFP. One correlate of this decrease in PV+ neuron recruitment is a substantial increase in the magnitude of the VEP elicited by the familiar stimulus. These observations are consistent with the findings of a previous study by Kaplan et al.[10] showing that the pharmacogenetic silencing of PV+ neurons locally within V1 causes an increase in VEPs that mimics and occludes SRP. Conversely, optogenetic stimulation of the PV+ neurons reverses SRP expression in the VEP. Together, the data strongly suggest that expression of SRP in the VEP is entirely accounted for by differential recruitment of PV+ interneurons by familiar and novel visual stimuli.

What mechanism is responsible for loss of PV+ cell activation by a familiar stimulus? In layer 4 of sensory cortex, PV+ inhibitory neurons are known to be strongly inhibited by SOM+ neurons[43,44]. Inspired by these findings and a study in auditory cortex showing that passive sound exposure upregulates SOM+ neuron activity in layer 3[19], we examined the effect of visual grating familiarity on the activity of SOM+ neurons in layer 4 of V1. The data show a robust and strikingly uniform increase in the activity of SOM+ cells as the stimulus becomes familiar. As expected from previous work[38], engagement of SOM+ cells by the familiar stimulus was clearly reflected in the LFP which showed a dramatic increase in the power and duration of low-frequency oscillations. This is the dominant processing mode for familiar stimuli in V1 of awake mice (**Figure 11**). As a novel stimulus becomes familiar and a memory is formed, increased engagement of the SOM+ cell network suppresses PV+ cells, decreases high-frequency oscillations, and increases VEPs in layer 4.

The observed shifts in oscillations and inhibitory networks are not accounted for by movement or global state changes

Although the mice in our study were restrained, they were free to move the forepaws. Previous studies have shown that this movement increases briefly (for approximately 5 sec) following the transition from a gray screen to a novel grating (a response called a vidget) and that it habituates over days as the grating becomes familiar[7,9,10]. However, continuous monitoring of forepaw movement over the entire block of phase-reversing stimuli showed no familiar-novel differences, suggesting that movement is not a confounding variable for the interpretation of our LFP or imaging data. Indeed, although it has been shown by others that activity of SOM+ and PV+ neurons of mouse V1 is strongly modulated by locomotion[32], both populations in layer 4 show comparable and uniform increases when movement occurs during visual stimulation[45]. Thus, the differential recruitment of these inhibitory networks by familiar and novel stimuli is unlikely to be accounted for by differences in movement.

Cortical responsiveness is known to be modulated by transitions in global brain states that are mediated by diffusely projecting neuromodulatory systems[31,46,47]. In principle, our findings could be explained if novel stimuli produce more sustained arousal than do familiar stimuli. Arousal and global modulation can be monitored via measurement of pupil size[33,34]; however, we detected no differences in pupil size during familiar or novel stimulus presentation. Furthermore, an expression mechanism that depends on slowly conducting modulatory systems seems unlikely considering (1) the speed of the transition in the LFP that heralds familiarity recognition and (2) the fact that the essential synaptic modifications underlying SRP induction and maintenance reside within V1.

A previous study of mouse V1 reported interesting changes in LFP oscillations in V1 that varied with stimulus familiarity[6]. However, a number of methodological and analytic differences make comparisons with the current work difficult. In the study by Kissinger et al.[6], presentation of a moving or static grating stimulus elicited a VEP that developed strong oscillations in all frequency bands, including gamma, as the stimulus became familiar. These oscillations were most prominent at the theta frequency (4-8 Hz), and the ringing of the VEP could last for up to 1 second. Although the amplitude was reduced, the same frequency oscillations were apparent when a novel stimulus orientation was presented. A potential confound is that Kissinger et al. spectrally analyzed periods of the LFP containing the VEP, whereas we specifically have not due to the violation of second-order stationarity. In any case, expression of the phenomena they described was sensitive to inhibition of modulatory cholinergic input to V1, and correlated with changes in pupil size, suggesting participation of very different mechanisms than those engaged in the context of SRP.

Recognition occurs rapidly and is reinforced by repetitive stimulation

There is no discernable familiar-novel difference between VEPs elicited by the transition from a gray screen to an oriented grating[36]. This finding and others[8,9] suggest that the memory of stimulus familiarity is not simply encoded by enhanced monosynaptic thalamocortical transmission in layer 4. Rather, recognition emerges with time as the stimuli are presented. During the train of stimuli, VEPs to familiar stimuli exhibit less adaptation than the VEPs to novel stimuli. This finding is consistent with the concept of reentrant recruitment of different inhibitory networks[48]. Calcium imaging does not provide the temporal resolution to resolve the timing of this signature of recognition, but the VEP and LFP yield some additional insight. The familiar-novel difference in the low-frequency oscillations is significant as soon as the LFP can be unambiguously analyzed, 0.5 s after the first phase reversal. Similarly, the VEP is clearly potentiated by the phase reversal of a familiar stimulus relative to novel 0.5 s after the transition from gray screen. These findings indicate that a familiar stimulus recruits the SOM+ neurons within a half-second, potentiating the VEPs by suppressing the PV+ neurons. Our data are consistent with the findings of a previous study, showing that recognition of stimulus orientation in a V1-dependent operant task can occur very rapidly, within 80 ms of stimulus onset[49].

Interestingly, during the train of phase reversals of a familiar stimulus we observe a modulation in the power of the low-frequency oscillations, increasing just before each phase transition. There is evidence from monkey studies that top-down or feedback inputs elicit low-frequency oscillations in V1[50] and that these are prominent when sensory stimuli are predictable[51]. Experiments in mice also show that the activity of SOM+ neurons in layer 3 of visual cortex is influenced by top-down input[37]. Although a substantial body of evidence indicates that induction and maintenance of the synaptic modifications responsible for SRP occur locally within V1[7,8], this does not preclude a contribution of top-down modulation in the expression mechanism. An interesting possibility is that such feedback is involved specifically in the prediction of stimulus timing that is revealed by the anticipatory increases in low-frequency oscillations between regularly spaced phase reversals.

Exposure to a novel grating orientation triggers persistent oscillations in V1

Novelty is a major driver of orienting, exploration, and visual attention[52-54]. Given reports that implicate visual cortical gamma oscillations in visual attentional processes[55-57], the emergence of high frequency oscillations with novel grating orientations is not surprising. Gamma oscillations

and PV+ cells influence cortical function to provide maximal feature detection[58-60] and selectivity[61] to improve object representation[62]. Gamma oscillations additionally contribute to learning and memory processes in visual cortex[63,64] and maximize information acquisition[65], consistent with our observations that these are at their peak during the initial exposure to a visual stimulus that will result in experience-dependent plasticity. It is noteworthy that although novel stimuli elicit smaller VEPs than familiar stimuli, calcium imaging of layer 4 principal neurons reveals much stronger responses to novel orientations than to familiar[36]. These calcium signals reflect changes in sustained activity of layer 4 neurons, as they do not report the augmentation in peak spiking rates that occur with each phase reversal of a familiar stimulus[3,7,66]. Nevertheless, the calcium responses of these neurons parallel the reflexive behavioral response to novelty, which is pronounced initially but shows long-term habituation as the stimulus becomes familiar[7].

While the increase in high-frequency oscillations with novel stimuli was expected, we were surprised to see an additional transient increase in the power of low-frequency oscillations. The data show that with a lag of ~2 sec, the low-frequency oscillations also increase during the novel stimulus train for about 30 sec before subsiding to baseline levels. Thus, the reciprocity of high- and low-frequency oscillations is not perfectly symmetrical. Strong recruitment of low-frequency oscillations by familiar stimuli appears to rapidly extinguish high-frequency oscillations, whereas strong recruitment of high-frequency oscillations by novel stimuli does not preclude a concurrent increase in low-frequency oscillations. These findings are compatible with the reported asymmetry in the connectivity of SOM+ and PV+ neurons. Whereas SOM+ neurons strongly inhibit PV+ neurons, the reverse modulation is far weaker[44].

Putting the pieces together

The current study adds important new pieces to the puzzle of SRP and visual recognition memory in V1. The original description of SRP was the robust increase in the magnitude of the VEP elicited by phase-reversing a familiar stimulus[1]. Current-source density analysis reveals that SRP of the VEP in layer 4 reflects a net increase in positive current flowing into (most likely) radially oriented apical dendrites[7]. Combined with our previous findings[10], the current results indicate that the simplest explanation for this increase in net current flow is reduced PV+ mediated inhibition. Moreover, in agreement with other reports in the literature[19,37], our findings suggest that the simplest explanation for the reduced PV+ cell activation by familiar stimuli is an experience-dependent increase in the activation of SOM+ neurons. However, a full description of SRP must also account for the additional observations that, when measured with calcium imaging, layer 4 principal cell activity is reduced during familiar stimulus viewing[36]. Similarly, the reflexive orienting response to the onset of a visual stimulus is reduced when the stimulus is familiar—behavioral plasticity that has the same mechanistic requirements as SRP in V1[67]. It is tempting to speculate that recruitment of SOM+ neurons by familiar stimuli could be responsible for multiple facets of SRP: suppression of both principal cell and PV+ activity in layer 4, as well as the behavioral response. This model depends on several assumptions that will be interesting to test in future studies. We are still left with the question of how SOM+ neurons become more active as a stimulus is learned. There are many possibilities that remain to be explored, but available data indicate there is an essential role for mechanisms of excitatory synaptic plasticity that are shared by the phenomenon of LTP[2,8].

The data suggest that the PV+ neurons, which are known to receive a more powerful thalamic input than glutamatergic principal neurons[68], are highly engaged by unexpected feedforward sensory input, while SOM+ neurons are recruited by a recognition memory trace

within V1[1,2,7]. Thus, the novelty response may reflect a default feedforward state that remains unhindered until a stimulus is recognized as familiar. This putative organization is similar conceptually to the comparator model of habituation[69], in which sensory input is constantly compared to engrams distributed throughout the cortex and only when a match occurs is inhibition recruited to suppress reflexive behavioral output. The comparator model contrasts with the more commonly invoked adaptive filtration/dual process theory[70], in which feedforward synaptic input is progressively weakened with repeated use, resulting in reduced activation and reduced output. Future studies aimed at dissecting the proposed interplay between these two inhibitory neuronal populations as they engage with familiarity or novelty processing, and the potential implementation of these circuits within comparator/adaptive filtration systems, will be of great interest.

Acknowledgements:

We acknowledge the invaluable support of Arnold Heynen, Suzanne Meagher, Nina Palisano, Jessica Buckey, Erik Sklar, Kiki Chu, Emily Greene-Colozzi, Amanda Coronado, Athene Wilson-Glover, and Erin Hickey throughout this study. We particularly thank Dr. Robert W. Komorowski for initiating and encouraging this project. Support was provided by the Howard Hughes Medical Institute, the National Institutes of Health (R01EY023037), the Picower Institute Innovation Fund, the Picower Young Faculty Support Fund (RWK), and a National Science Foundation Graduate Research Fellowship (DJH). SFC is funded by the Wellcome Trust (207727/Z/17/Z) and the Biotechnology and Biological Sciences Research Council (BB/S008276/1).

Correspondence:
Mark Bear
Department of Brain and Cognitive Sciences
Massachusetts Institute of Technology
Cambridge, MA, USA 02139
mbear@mit.edu

References:

1 Frenkel, M. Y. *et al.* Instructive effect of visual experience in mouse visual cortex. *Neuron* **51**, 339-349, doi:10.1016/j.neuron.2006.06.026 (2006).

2 Cooke, S. F. & Bear, M. F. Visual experience induces long-term potentiation in the primary visual cortex. *J Neurosci* **30**, 16304-16313, doi:10.1523/JNEUROSCI.4333-10.2010 (2010).

3 Aton, S. J., Suresh, A., Broussard, C. & Frank, M. G. Sleep promotes cortical response potentiation following visual experience. *Sleep* **37**, 1163-1170, doi:10.5665/sleep.3830 (2014).

4 Kaneko, M. & Stryker, M. P. Sensory experience during locomotion promotes recovery of function in adult visual cortex. *Elife* **3**, e02798, doi:10.7554/eLife.02798 (2014).

5 Kaneko, M., Fu, Y. & Stryker, M. P. Locomotion Induces Stimulus-Specific Response Enhancement in Adult Visual Cortex. *J Neurosci* **37**, 3532-3543, doi:10.1523/JNEUROSCI.3760-16.2017 (2017).

6 Kissinger, S. T., Pak, A., Tang, Y., Masmanidis, S. C. & Chubykin, A. A. Oscillatory Encoding of Visual Stimulus Familiarity. *J Neurosci* **38**, 6223-6240, doi:10.1523/JNEUROSCI.3646-17.2018 (2018).
7 Cooke, S. F., Komorowski, R. W., Kaplan, E. S., Gavornik, J. P. & Bear, M. F. Visual recognition memory, manifested as long-term habituation, requires synaptic plasticity in V1. *Nature neuroscience* **18**, 262-271, doi:10.1038/nn.3920 (2015).
8 Cooke, S. F. & Bear, M. F. How the mechanisms of long-term synaptic potentiation and depression serve experience-dependent plasticity in primary visual cortex. *Philos Trans R Soc Lond B Biol Sci* **369**, 20130284, doi:10.1098/rstb.2013.0284 (2014).
9 Fong, M. F. *et al.* Distinct Laminar Requirements for NMDA Receptors in Experience-Dependent Visual Cortical Plasticity. *Cereb Cortex* **30**, 2555-2572, doi:10.1093/cercor/bhz260 (2020).
10 Kaplan, E. S. *et al.* Contrasting roles for parvalbumin-expressing inhibitory neurons in two forms of adult visual cortical plasticity. *Elife* **5**, doi:10.7554/eLife.11450 (2016).
11 Cardin, J. A. *et al.* Driving fast-spiking cells induces gamma rhythm and controls sensory responses. *Nature* **459**, 663-667, doi:10.1038/nature08002 (2009).
12 Korotkova, T., Fuchs, E. C., Ponomarenko, A., von Engelhardt, J. & Monyer, H. NMDA receptor ablation on parvalbumin-positive interneurons impairs hippocampal synchrony, spatial representations, and working memory. *Neuron* **68**, 557-569, doi:10.1016/j.neuron.2010.09.017 (2010).
13 Carlen, M. *et al.* A critical role for NMDA receptors in parvalbumin interneurons for gamma rhythm induction and behavior. *Molecular psychiatry* **17**, 537-548, doi:10.1038/mp.2011.31 (2012).
14 Gonzalez-Burgos, G. & Lewis, D. A. NMDA receptor hypofunction, parvalbumin-positive neurons, and cortical gamma oscillations in schizophrenia. *Schizophr Bull* **38**, 950-957, doi:10.1093/schbul/sbs010 (2012).
15 Lewis, D. A., Curley, A. A., Glausier, J. R. & Volk, D. W. Cortical parvalbumin interneurons and cognitive dysfunction in schizophrenia. *Trends Neurosci* **35**, 57-67, doi:10.1016/j.tins.2011.10.004 (2012).
16 Kuki, T. *et al.* Contribution of parvalbumin and somatostatin-expressing GABAergic neurons to slow oscillations and the balance in beta-gamma oscillations across cortical layers. *Front Neural Circuits* **9**, 6, doi:10.3389/fncir.2015.00006 (2015).
17 Jadi, M. P., Behrens, M. M. & Sejnowski, T. J. Abnormal Gamma Oscillations in N-Methyl-D-Aspartate Receptor Hypofunction Models of Schizophrenia. *Biol Psychiatry* **79**, 716-726, doi:10.1016/j.biopsych.2015.07.005 (2016).
18 Polepalli, J. S. *et al.* Modulation of excitation on parvalbumin interneurons by neuroligin-3 regulates the hippocampal network. *Nature neuroscience* **20**, 219-229, doi:10.1038/nn.4471 (2017).
19 Kato, H. K., Gillet, S. N. & Isaacson, J. S. Flexible Sensory Representations in Auditory Cortex Driven by Behavioral Relevance. *Neuron* **88**, 1027-1039, doi:10.1016/j.neuron.2015.10.024 (2015).
20 Mathis, A. *et al.* DeepLabCut: markerless pose estimation of user-defined body parts with deep learning. *Nature neuroscience* **21**, 1281-1289, doi:10.1038/s41593-018-0209-y (2018).

21 Bokil, H., Andrews, P., Kulkarni, J. E., Mehta, S. & Mitra, P. P. Chronux: a platform for analyzing neural signals. *J Neurosci Methods* **192**, 146-151, doi:10.1016/j.jneumeth.2010.06.020 (2010).
22 Caplan, J. B., Madsen, J. R., Raghavachari, S. & Kahana, M. J. Distinct patterns of brain oscillations underlie two basic parameters of human maze learning. *Journal of neurophysiology* **86**, 368-380, doi:10.1152/jn.2001.86.1.368 (2001).
23 van Vugt, M. K., Sederberg, P. B. & Kahana, M. J. Comparison of spectral analysis methods for characterizing brain oscillations. *J Neurosci Methods* **162**, 49-63, doi:10.1016/j.jneumeth.2006.12.004 (2007).
24 Pachitariu, M. *et al.* Suite2p: beyond 10,000 neurons with standard two-photon microscopy. *bioRxiv*, 061507, doi:10.1101/061507 (2017).
25 Chen, T. W. *et al.* Ultrasensitive fluorescent proteins for imaging neuronal activity. *Nature* **499**, 295-300, doi:10.1038/nature12354 (2013).
26 Saravanan, V., Berman, G. J. & Sober, S. J. Application of the Hierarchical Bootstrap to Multi-Level Data in Neuroscience. *bioRxiv*, 819334, doi:10.1101/819334 (2020).
27 Chalk, M. *et al.* Attention reduces stimulus-driven gamma frequency oscillations and spike field coherence in V1. *Neuron* **66**, 114-125, doi:10.1016/j.neuron.2010.03.013 (2010).
28 Zhou, H., Schafer, R. J. & Desimone, R. Pulvinar-Cortex Interactions in Vision and Attention. *Neuron* **89**, 209-220, doi:10.1016/j.neuron.2015.11.034 (2016).
29 Saleem, A. B. *et al.* Subcortical Source and Modulation of the Narrowband Gamma Oscillation in Mouse Visual Cortex. *Neuron* **93**, 315-322, doi:10.1016/j.neuron.2016.12.028 (2017).
30 Niell, C. M. & Stryker, M. P. Modulation of visual responses by behavioral state in mouse visual cortex. *Neuron* **65**, 472-479, doi:10.1016/j.neuron.2010.01.033 (2010).
31 Bennett, C., Arroyo, S. & Hestrin, S. Subthreshold mechanisms underlying state-dependent modulation of visual responses. *Neuron* **80**, 350-357, doi:10.1016/j.neuron.2013.08.007 (2013).
32 Fu, Y. *et al.* A cortical circuit for gain control by behavioral state. *Cell* **156**, 1139-1152, doi:10.1016/j.cell.2014.01.050 (2014).
33 Reimer, J. *et al.* Pupil fluctuations track fast switching of cortical states during quiet wakefulness. *Neuron* **84**, 355-362, doi:10.1016/j.neuron.2014.09.033 (2014).
34 Vinck, M., Batista-Brito, R., Knoblich, U. & Cardin, J. A. Arousal and locomotion make distinct contributions to cortical activity patterns and visual encoding. *Neuron* **86**, 740-754, doi:10.1016/j.neuron.2015.03.028 (2015).
35 Reimer, J. *et al.* Pupil fluctuations track rapid changes in adrenergic and cholinergic activity in cortex. *Nat Commun* **7**, 13289, doi:10.1038/ncomms13289 (2016).
36 Kim, T., Chaloner, F. A., Cooke, S. F., Harnett, M. T. & Bear, M. F. Opposing Somatic and Dendritic Expression of Stimulus-Selective Response Plasticity in Mouse Primary Visual Cortex. *Front Cell Neurosci* **13**, 555, doi:10.3389/fncel.2019.00555 (2019).
37 Makino, H. & Komiyama, T. Learning enhances the relative impact of top-down processing in the visual cortex. *Nature neuroscience* **18**, 1116-1122, doi:10.1038/nn.4061 (2015).
38 Chen, G. *et al.* Distinct Inhibitory Circuits Orchestrate Cortical beta and gamma Band Oscillations. *Neuron* **96**, 1403-1418 e1406, doi:10.1016/j.neuron.2017.11.033 (2017).

39 Khan, A. G. *et al.* Distinct learning-induced changes in stimulus selectivity and interactions of GABAergic interneuron classes in visual cortex. *Nature neuroscience* **21**, 851-859, doi:10.1038/s41593-018-0143-z (2018).
40 Hamm, J. P. & Yuste, R. Somatostatin Interneurons Control a Key Component of Mismatch Negativity in Mouse Visual Cortex. *Cell Rep* **16**, 597-604, doi:10.1016/j.celrep.2016.06.037 (2016).
41 Rankin, C. H. *et al.* Habituation revisited: an updated and revised description of the behavioral characteristics of habituation. *Neurobiology of learning and memory* **92**, 135-138, doi:10.1016/j.nlm.2008.09.012 (2009).
42 Ramaswami, M. Network plasticity in adaptive filtering and behavioral habituation. *Neuron* **82**, 1216-1229, doi:10.1016/j.neuron.2014.04.035 (2014).
43 Xu, H., Jeong, H. Y., Tremblay, R. & Rudy, B. Neocortical somatostatin-expressing GABAergic interneurons disinhibit the thalamorecipient layer 4. *Neuron* **77**, 155-167, doi:10.1016/j.neuron.2012.11.004 (2013).
44 Pfeffer, C. K., Xue, M., He, M., Huang, Z. J. & Scanziani, M. Inhibition of inhibition in visual cortex: the logic of connections between molecularly distinct interneurons. *Nature neuroscience* **16**, 1068-1076, doi:10.1038/nn.3446 (2013).
45 Pakan, J. M. *et al.* Behavioral-state modulation of inhibition is context-dependent and cell type specific in mouse visual cortex. *Elife* **5**, doi:10.7554/eLife.14985 (2016).
46 Hasenstaub, A., Sachdev, R. N. & McCormick, D. A. State changes rapidly modulate cortical neuronal responsiveness. *J Neurosci* **27**, 9607-9622, doi:10.1523/JNEUROSCI.2184-07.2007 (2007).
47 Luczak, A., Bartho, P. & Harris, K. D. Gating of sensory input by spontaneous cortical activity. *J Neurosci* **33**, 1684-1695, doi:10.1523/JNEUROSCI.2928-12.2013 (2013).
48 Sporns, O., Gally, J. A., Reeke, G. N., Jr. & Edelman, G. M. Reentrant signaling among simulated neuronal groups leads to coherency in their oscillatory activity. *Proceedings of the National Academy of Sciences of the United States of America* **86**, 7265-7269, doi:10.1073/pnas.86.18.7265 (1989).
49 Resulaj, A., Ruediger, S., Olsen, S. R. & Scanziani, M. First spikes in visual cortex enable perceptual discrimination. *Elife* **7**, doi:10.7554/eLife.34044 (2018).
50 van Kerkoerle, T. *et al.* Alpha and gamma oscillations characterize feedback and feedforward processing in monkey visual cortex. *Proceedings of the National Academy of Sciences of the United States of America* **111**, 14332-14341, doi:10.1073/pnas.1402773111 (2014).
51 Bastos, A. M., Lundqvist, M., Waite, A. S., Kopell, N. & Miller, E. K. Layer and rhythm specificity for predictive routing. *Proceedings of the National Academy of Sciences of the United States of America* **117**, 31459-31469, doi:10.1073/pnas.2014868117 (2020).
52 Barry, R. J. Habituation of the orienting reflex and the development of Preliminary Process Theory. *Neurobiology of learning and memory* **92**, 235-242, doi:10.1016/j.nlm.2008.07.007 (2009).
53 Itti, L. & Baldi, P. Bayesian surprise attracts human attention. *Vision Res* **49**, 1295-1306, doi:10.1016/j.visres.2008.09.007 (2009).
54 Gottlieb, J., Oudeyer, P. Y., Lopes, M. & Baranes, A. Information-seeking, curiosity, and attention: computational and neural mechanisms. *Trends in cognitive sciences* **17**, 585-593, doi:10.1016/j.tics.2013.09.001 (2013).

55 Fries, P., Reynolds, J. H., Rorie, A. E. & Desimone, R. Modulation of oscillatory neuronal synchronization by selective visual attention. *Science* **291**, 1560-1563, doi:10.1126/science.1055465 (2001).
56 Tiesinga, P. H., Fellous, J. M., Salinas, E., Jose, J. V. & Sejnowski, T. J. Inhibitory synchrony as a mechanism for attentional gain modulation. *Journal of physiology, Paris* **98**, 296-314, doi:10.1016/j.jphysparis.2005.09.002 (2004).
57 Borgers, C., Epstein, S. & Kopell, N. J. Background gamma rhythmicity and attention in cortical local circuits: a computational study. *Proceedings of the National Academy of Sciences of the United States of America* **102**, 7002-7007, doi:10.1073/pnas.0502366102 (2005).
58 Lee, S. H. *et al.* Activation of specific interneurons improves V1 feature selectivity and visual perception. *Nature* **488**, 379-383, doi:10.1038/nature11312 (2012).
59 Siegle, J. H., Pritchett, D. L. & Moore, C. I. Gamma-range synchronization of fast-spiking interneurons can enhance detection of tactile stimuli. *Nature neuroscience* **17**, 1371-1379, doi:10.1038/nn.3797 (2014).
60 Speed, A., Del Rosario, J., Burgess, C. P. & Haider, B. Cortical State Fluctuations across Layers of V1 during Visual Spatial Perception. *Cell Rep* **26**, 2868-2874 e2863, doi:10.1016/j.celrep.2019.02.045 (2019).
61 Womelsdorf, T. *et al.* Orientation selectivity and noise correlation in awake monkey area V1 are modulated by the gamma cycle. *Proceedings of the National Academy of Sciences of the United States of America* **109**, 4302-4307, doi:10.1073/pnas.1114223109 (2012).
62 Rotermund, D., Taylor, K., Ernst, U. A., Kreiter, A. K. & Pawelzik, K. R. Attention improves object representation in visual cortical field potentials. *J Neurosci* **29**, 10120-10130, doi:10.1523/JNEUROSCI.5508-08.2009 (2009).
63 Osipova, D. *et al.* Theta and gamma oscillations predict encoding and retrieval of declarative memory. *J Neurosci* **26**, 7523-7531, doi:10.1523/JNEUROSCI.1948-06.2006 (2006).
64 Jokisch, D. & Jensen, O. Modulation of gamma and alpha activity during a working memory task engaging the dorsal or ventral stream. *J Neurosci* **27**, 3244-3251, doi:10.1523/JNEUROSCI.5399-06.2007 (2007).
65 Pritchett, D. L., Siegle, J. H., Deister, C. A. & Moore, C. I. For things needing your attention: the role of neocortical gamma in sensory perception. *Curr Opin Neurobiol* **31**, 254-263, doi:10.1016/j.conb.2015.02.004 (2015).
66 Clawson, B. C. *et al.* Sleep Promotes, and Sleep Loss Inhibits, Selective Changes in Firing Rate, Response Properties and Functional Connectivity of Primary Visual Cortex Neurons. *Front Syst Neurosci* **12**, 40, doi:10.3389/fnsys.2018.00040 (2018).
67 Cooke, S. F. & Bear, M. F. Visual recognition memory: a view from V1. *Curr Opin Neurobiol* **35**, 57-65, doi:10.1016/j.conb.2015.06.008 (2015).
68 Cruikshank, S. J., Lewis, T. J. & Connors, B. W. Synaptic basis for intense thalamocortical activation of feedforward inhibitory cells in neocortex. *Nature neuroscience* **10**, 462-468, doi:10.1038/nn1861 (2007).
69 Sokolov, E. N. Higher nervous functions; the orienting reflex. *Annual review of physiology* **25**, 545-580, doi:10.1146/annurev.ph.25.030163.002553 (1963).
70 Groves, P. M. & Thompson, R. F. Habituation: a dual-process theory. *Psychol Rev* **77**, 419-450, doi:10.1037/h0029810 (1970).

Figure Legends:

Figure 1 – Layer 4 local field potential displays variable frequency composition in V1 of awake, head-fixed mice: (**A**) We recorded local field potentials (LFP) from primary visual cortex (V1) in awake, head-fixed mice in response to phase-reversing sinusoidal grating stimuli. (**B**) Electrodes were chronically implanted bilaterally in thalamo-recipient layer 4 of binocular V1. (**C**) The experimental set-up (see Methods). (**D**) Examination of the continuous LFP (black trace) relative to each phase-reversal (gray and white slanted bars) reveals marked variability in V1 activity given the consistency of the visual stimulus. Blue and cyan colored outlines around a visual stimulus identify each phase-reversal as either phase 0° ("flip") or phase 180° ("flop"). The dashed black line connecting the time series trace with the spectrogram indicates the period of time spectral analysis was conducted on. (**E**) The raw spectrogram for the periods outlined in (**D**). (**F**) The normalized spectrogram for the periods outlined in (**D**).

Figure 2 – V1 oscillations are influenced by stimulus familiarity over days: (**A**) In 13 mice, repeated presentation of the same stimulus orientation over 6 days increases low frequency power and decreases high frequency power. Averaged spectrums are presented as mean +/- SEM. (**B**) Non-parametric hierarchical bootstrapping results confirm that the spectrum on day 6 (blue) is significantly different from the spectrum on day 1 (cyan), despite the fact the stimulus has not changed. Solid line represents the median value and the shaded region reflects the 99% confidence interval. (**C**) Same as in (**A**), but focused on the amount of time the local field potential shows sustained oscillatory activity for a given band. (**D**) Same as in (**B**), but focused on the amount of time the local field potential shows sustained oscillatory activity for a given band. Marks near the x-axis in (**B**) and (**D**) indicate the 99% confidence interval does not include 0 (thus the difference is statistically significant).

Figure 3 – Experience-dependent oscillations in V1 are stimulus-specific: (**A**) In 13 mice, presentation of a novel (red) stimulus causes increased high frequency power and decreased low frequency power compared to a familiar (blue) stimulus. Averaged spectrums are presented as mean +/- SEM. (**B**) Non-parametric hierarchical bootstrapping results confirm that the familiar spectrum is significantly different from the novel spectrum. Solid line represents the median value and the shaded region reflects the 99% confidence interval. (**C**) Same as in (**A**), but focused on the amount of time the local field potential shows sustained oscillatory activity for a given band. (**D**) Same as in (**B**), but focused on the amount of time the local field potential shows sustained oscillatory activity for a given band. Marks near the x-axis in (**B**) and (**D**) indicate the 99% confidence interval does not include 0 (thus the difference is statistically significant).

Figure 4 – Arousal does not account for the changes in layer 4 LFP frequency composition: (**A**) We recorded piezo-electric activity from the forepaws of awake, head-fixed mice in response to phase-reversing sinusoidal grating stimuli. (**B**) In 5 mice, the normalized piezo-electric voltage (see Methods) indicates there is no difference in the forepaw movement between familiar and novel stimuli. Averaged voltages are presented as mean +/- SEM. (**C**) Non-parametric hierarchical bootstrapping results confirm that there is no piezo-electric voltage difference between familiar and novel stimuli. (**D**) We recorded animal's pupils while they viewed familiar

and novel stimuli. An example familiar and novel frame show the average size of the pupil. (**E**) In 4 mice, the pupil diameter is similar between familiar and novel stimuli. Averaged pupil diameters are presented as mean +/- SEM. (**F**) Non-parametric hierarchical bootstrapping results confirm that there is no pupil diameter difference between familiar and novel stimuli.

Figure 5 – Oscillations and VEP magnitude correlate: (**A**) LFPs and VEPs proximal to 500 stimulus phase reversals were studied in 13 mice. The max low frequency (10-30 Hz) power is larger for familiar stimuli than novel stimuli. (**B**) The max high frequency (60-80 Hz) power is larger for novel stimuli than familiar stimuli. (**C**) The VEP magnitude is larger for familiar stimuli than novel stimuli. (**D**) An exemplar animal's scatterplot of each presentation's max low frequency power and high frequency power shows they are negatively correlated. (**E**) Non-parametric hierarchical bootstrapping results confirm that low frequency and high frequency power are negatively correlated, regardless of stimulus. (**F**) Same as in (**D**), but for low frequency power and VEP magnitude. (**G**) Same as in (**E**), but showing low frequency power positively correlates with VEP magnitude. (**H**) Same as in (**D**), but for high frequency power and VEP magnitude. (**I**) Same as in (**E**), but showing high frequency power negatively correlates with VEP magnitude. Solid lines in (**E**), (**G**), and (**I**) indicate the median value and the shaded region reflects the 99% confidence interval. "Both" refers to a correlation analysis done with equal random sampling of both familiar and novel stimulus presentations. Squares in (**D**), (**F**), and (**H**) represent the midpoint of each group's scatterplot cloud.

Figure 6 – Experience-dependent oscillations in V1 change within a block: (**A**) In 13 mice, the first phase ("flip") of a familiar stimulus block (cyan) has increased high frequency power and decreased low frequency power compared to the last presentation of the same phase stimulus (blue). Averaged spectrums are presented as mean +/- SEM. (**B**) Non-parametric hierarchical bootstrapping results confirm that the last flip's spectrum is significantly different from the first flip's spectrum. Solid line represents the median value and the shaded region reflects the 99% confidence interval. (**C**) The first flip of a novel stimulus block (magenta) has increased high frequency power compared to the last flip (red). (**D**) Same as in (**B**), but focused on novel block's first and last flip. (**E**) The max low frequency power near block onset increases to a higher value for familiar stimuli compared to novel stimuli. Gray vertical bars represent periods where the LFP is contaminated by the VEP so interpolation was done to connect non-contaminated regions of the plot (see Methods). Averaged power is presented as mean +/- SEM. (**F**) Non-parametric hierarchical bootstrapping results confirm that familiar stimuli have more low frequency power than novel. (**G**) Max high frequency power near block onset increases to a larger value for a novel stimulus than a familiar one. (**H**) Same as in (**F**), but focused on high frequency power at block onset. Marks near the x-axis in (**B**), (**D**) , (**E**), and (**F**) indicate the 99% confidence interval does not include 0 (thus the difference is statistically significant).

Figure 7 – Experience-dependent oscillations in V1 emerge over a few presentations: (**A**) In 13 mice, the average concatenated spectrum (see Methods) reveals short-term dynamics in oscillatory power for both familiar and novel stimuli. (**B**) For familiar stimuli, the max power in the 10-30 Hz band quickly increases to a steady value after the first presentation. Averaged power is presented as mean +/- SEM and the dashed blue line represents the average of the max power in the last 75 phase-reversals. (**C**) Non-parametric hierarchical bootstrapping results confirm that only the first presentation shows significantly different changes from the average of

the max power in the last 75 phase-reversals. Solid line represents the median value and the shaded region reflects the 99% confidence interval. (**D-E**) Same as (**B-C**), but showing, for familiar stimuli, that the max power in the 60-80 Hz band quickly decreases to a steady state value after the first presentation. (**F**) For novel stimuli, the max power in the 10-30 Hz band (magenta) rises during the 2nd through 5th presentations and slowly decays over the next 5-10 presentations. Averaged power is presented as mean +/- SEM and the dashed red line represents the average of the max power in the last 75 phase-reversals. (**G**) Non-parametric hierarchical bootstrapping results confirm the significantly different spectral changes from the average of the max power in the last 75 phase-reversals outlined in (**F**). Solid line represents the median value and the shaded region reflects the 99% confidence interval. (**H-I**) Same as (**F-G**), but showing, for novel stimuli, that the max power in the 60-80 Hz band decreases to a steady state value after the first few presentations. Marks near the x-axis in (**C**), (**E**), (**G**), and (**I**) indicate the 99% confidence interval does not include 0 (thus the difference is statistically significant).

Figure 8 – Experience-dependent oscillations in V1 change within a phase-reversal: (**A**) In 13 mice, only looking at the last 75 trials of each block, the average spectrogram shows timing dependent changes in oscillatory power for both familiar and novel stimuli. The early portion of a stimulus presentation is the average spectrogram between 400 and 1200 ms. The late portion of a stimulus presentation is the average spectrogram between 1200 and 2000 ms. (**B**) Non-parametric hierarchical bootstrapping results confirm that the late portion of a familiar presentation has significantly more power in the low frequency (10-30 Hz) range compared to the early portion. Solid line represents the median value and the shaded region reflects the 99% confidence interval. (**C**) Non-parametric hierarchical bootstrapping results confirm that the late portion of a novel presentation has significantly less power in the high frequency (60-80 Hz) range compared to the early portion. Solid line represents the median value and the shaded region reflects the 99% confidence interval. Marks near the x-axis in (**B**) and (**C**) indicate the 99% confidence interval does not include 0 (thus the difference is statistically significant).

Figure 9 – Layer 4 parvalbumin-expressing neurons are more active during novel stimuli compared to familiar stimuli whereas somatostatin-expressing neurons show the opposite effect: (**A**) We recorded parvalbumin-expressing (PV+) cell activity or somatostatin-expressing (SOM+) cell activity from layer 4 of V1 in awake, head-fixed mice in response to phase-reversing sinusoidal grating stimuli. (**B**) Image shows an example field of view (scale bar, 100 μm). (**C**) In 9 mice, PV+ cell activity gradually diminishes with stimulus experience. (**D**) Non-parametric hierarchical bootstrapping results confirm day 4 had less activity than day 1. (**E**) On day 5, PV+ cell activity is elevated while the mouse views novel stimuli. (**F**) Non-parametric hierarchical bootstrapping results confirm familiar stimuli induce less PV+ cell activity than novel stimuli. (**G**) In 7 mice, SOM+ cell activity gradually increases with stimulus experience. (**H**) Non-parametric hierarchical bootstrapping results confirm day 4 had more activity than day 1. (**I**) On day 5, SOM+ cell activity is elevated while the mouse views familiar stimuli. (**J**) Non-parametric hierarchical bootstrapping results confirm familiar stimuli induce more SOM+ cell activity than novel stimuli. All data is reported relative to the average inter-block gray screen activity (see Methods). Activity is averaged across all cells for each animal and presented as the group mean +/- SEM in (**C**), (**E**), (**G**), and (**I**). Solid black lines in (**D**), (**F**), (**H**), and (**J**) indicate the median value for the difference and the shaded regions reflect the 99% confidence interval.

Figure 10 - Parvalbumin-expressing and somatostatin-expressing neurons show a remarkably consistent response: (**A**) We recorded parvalbumin-expressing (PV+) cell activity from layer 4 of V1 in awake, head-fixed mice in response to phase-reversing sinusoidal grating stimuli across multiple days. The response to a stimulus on day 1 was larger than their response to the same, albeit now familiar, stimulus on day 4. (**B**) On day 5, presenting a novel stimulus once more engaged PV+ cell activity. (**C**) We recorded somatostatin-expressing (SOM+) cell activity from layer 4 of V1 in awake, head-fixed mice in response to phase-reversing sinusoidal grating stimuli across multiple days. The response to a stimulus on day 1 was smaller than their response to the same, albeit now familiar, stimulus on day 4. (**B**) On day 5, presenting a novel stimulus did not excite SOM+ cell activity. All data is reported relative to the average inter-block gray screen activity (see Methods). Dashed line in (**A**-**D**) is the identity line y = x.

Figure 11 – Working model of experience-dependent changes in cortical circuitry: A proposal for which interneuron circuits are engaged during familiar or novel stimuli (and their mutual opposition). See text for details.

Supplementary Figure 1 – Median black spectrogram for normalized spectral analysis (**A**) We recorded local field potentials (LFP) from layer 4 of binocular primary visual cortex (V1) in awake, head-fixed mice in response to blocks of phase-reversing sinusoidal grating stimuli separated by periods of gray and black screen. The median spectrogram for a period of black screen activity corresponding to similar periods for phase-reversing grating stimuli displays the expected pink noise common in neural recordings, but otherwise reveals no other time-dependent dynamics in spectral power.

Supplementary Figure 2 – Animal breakdown shows oscillations and VEP magnitude correlate, but not in stimulus-specific ways, across most mice: (**A**) Scatterplots of max low frequency (10-30 Hz) power and max high frequency (60-80 Hz) power for 12 of the 13 mice (the 13th is the exemplar in **Figure 5D**). (**B**) Scatterplots of max low frequency power and VEP magnitude for 12 of the 13 mice (the 13th is the exemplar in **Figure 5F**). (**C**) Scatterplots of max high frequency power and VEP magnitude for 12 of the 13 mice (the 13th is the exemplar in **Figure 5H**).

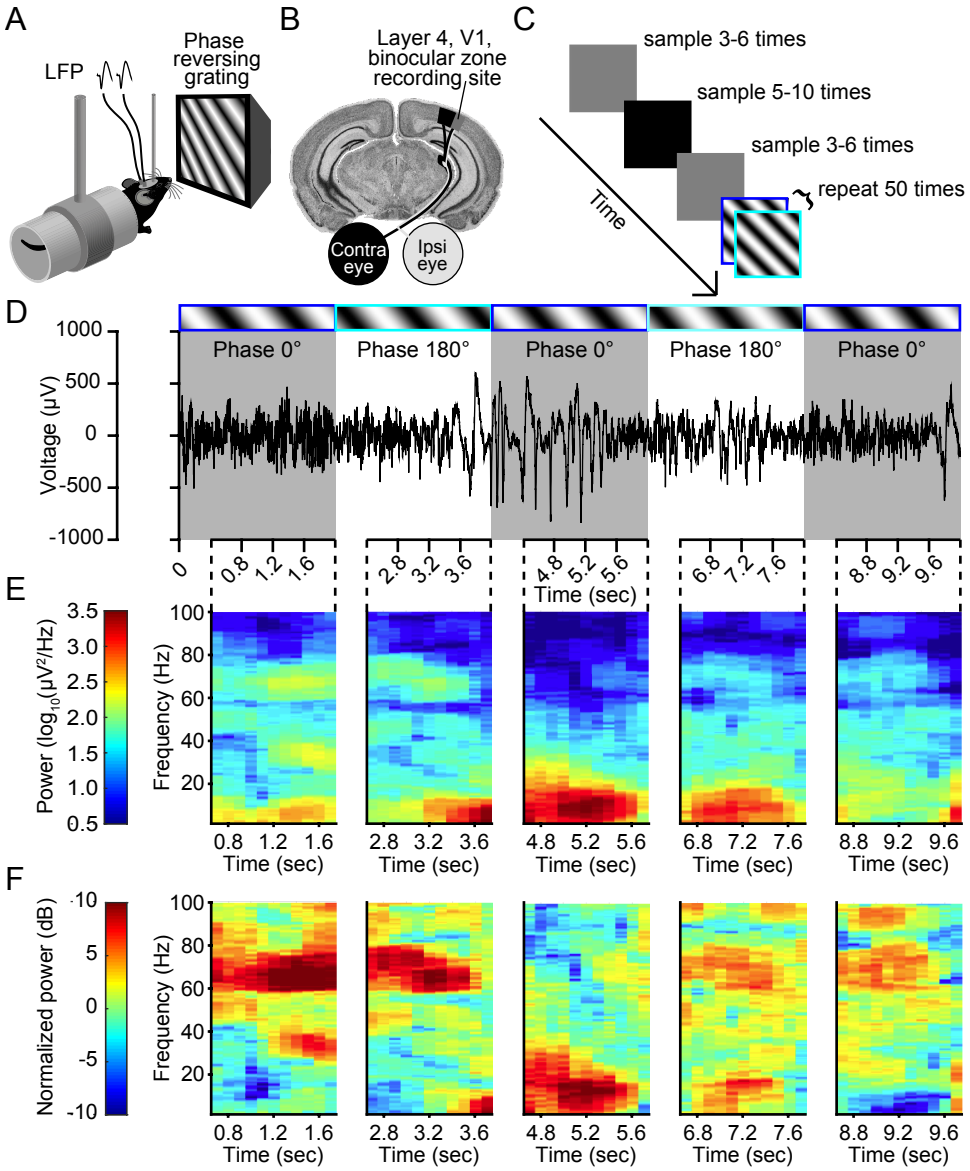
A
LFP
Phase reversing grating
B
Layer 4, V1, binocular zone recording site
Contra eye
Ipsi eye
C
sample 3-6 times
sample 5-10 times
sample 3-6 times
repeat 50 times
Time
D
Phase 0°
Phase 180°
Phase 0°
Phase 180°
Phase 0°
Voltage (μV)
1000
500
0
-500
-1000
0
0.8 1.2 1.6
2.8 3.2 3.6
4.8 5.2 5.6
6.8 7.2 7.6
8.8 9.2 9.6
Time (sec)
E
Power (log10(μV²/Hz))
3.5
3.0
2.5
2.0
1.5
1.0
0.5
Frequency (Hz)
100
80
60
40
20
0.8 1.2 1.6
2.8 3.2 3.6
4.8 5.2 5.6
6.8 7.2 7.6
8.8 9.2 9.6
Time (sec)
F
Normalized power (dB)
10
5
0
-5
-10
Frequency (Hz)
100
80
60
40
20
0.8 1.2 1.6
2.8 3.2 3.6
4.8 5.2 5.6
6.8 7.2 7.6
8.8 9.2 9.6
Time (sec)

Figure 2

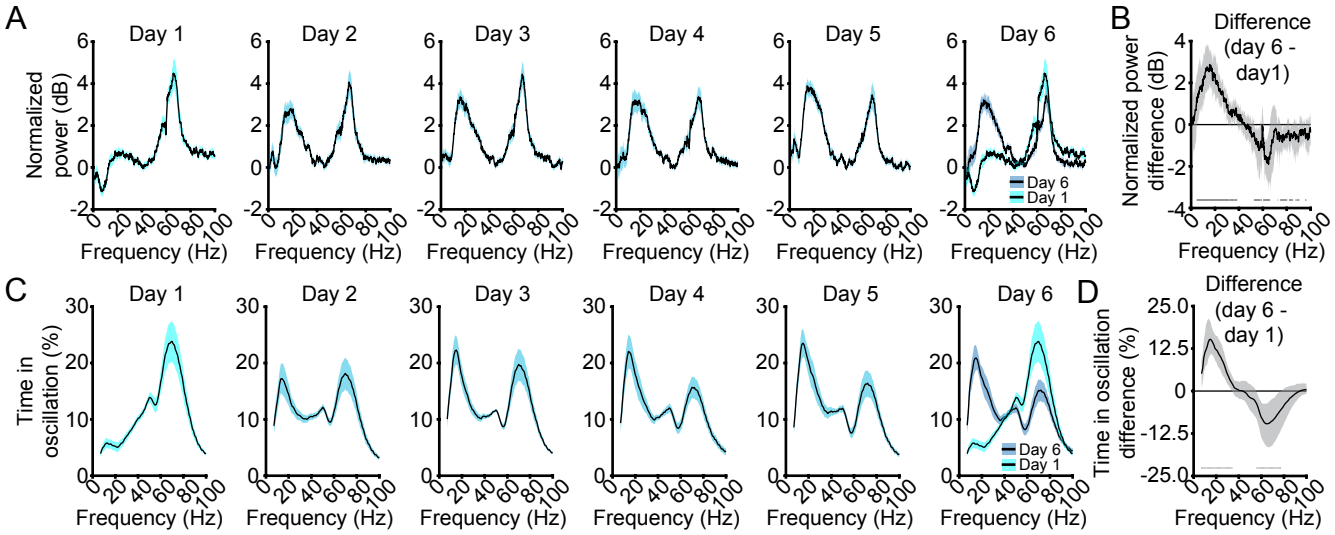
A
Day 1
Day 2
Day 3
Day 4
Day 5
Day 6
Normalized power (dB)
Frequency (Hz)
Day 6
Day 1
B
Difference (day 6 - day1)
Normalized power difference (dB)
Frequency (Hz)
C
Time in oscillation (%)
D
Difference (day 6 - day 1)
Time in oscillation difference (%)

Figure 3

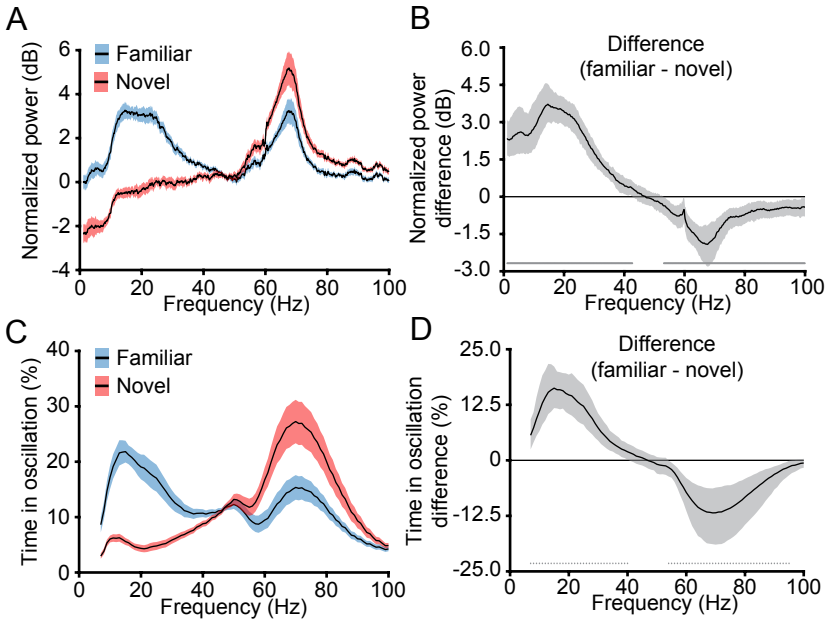
A
Familiar
Novel
Normalized power (dB)
6
4
2
0
-2
-4
0
20
40
60
80
100
Frequency (Hz)
B
Difference
(familiar - novel)
Normalized power
difference (dB)
6.0
4.5
3.0
1.5
0
-1.5
-3.0
0
20
40
60
80
100
Frequency (Hz)
C
Familiar
Novel
Time in oscillation (%)
40
30
20
10
0
0
20
40
60
80
100
Frequency (Hz)
D
Difference
(familiar - novel)
Time in oscillation
difference (%)
25.0
12.5
0
-12.5
-25.0
0
20
40
60
80
100
Frequency (Hz)

Figure 4

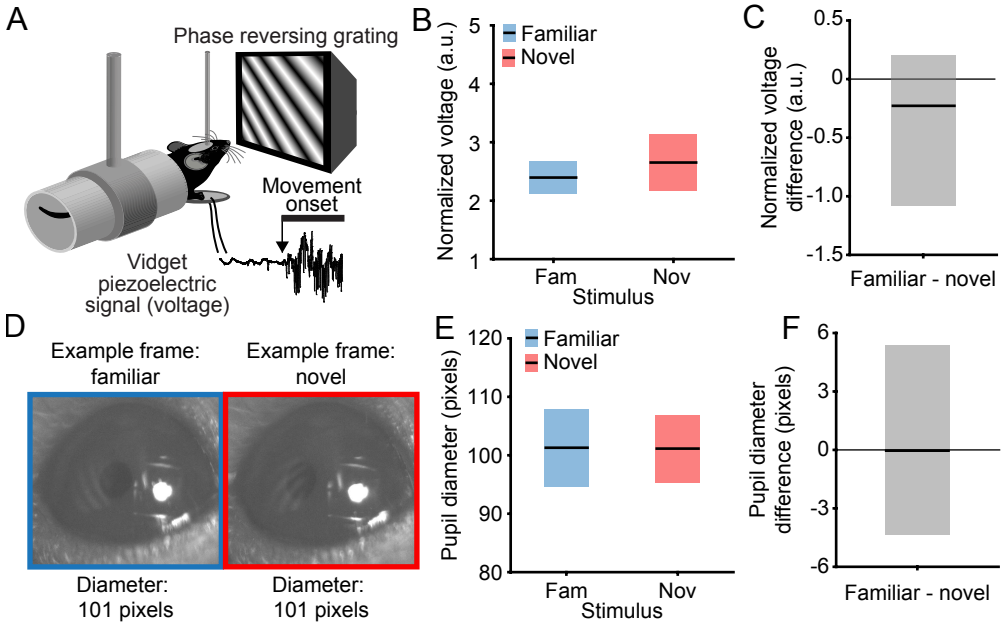
A
Phase reversing grating
Movement onset
Vidget piezoelectric signal (voltage)
B
Normalized voltage (a.u.)
Familiar
Novel
Fam
Nov
Stimulus
C
Normalized voltage difference (a.u.)
Familiar - novel
D
Example frame: familiar
Example frame: novel
Diameter: 101 pixels
Diameter: 101 pixels
E
Pupil diameter (pixels)
Familiar
Novel
Fam
Nov
Stimulus
F
Pupil diameter difference (pixels)
Familiar - novel

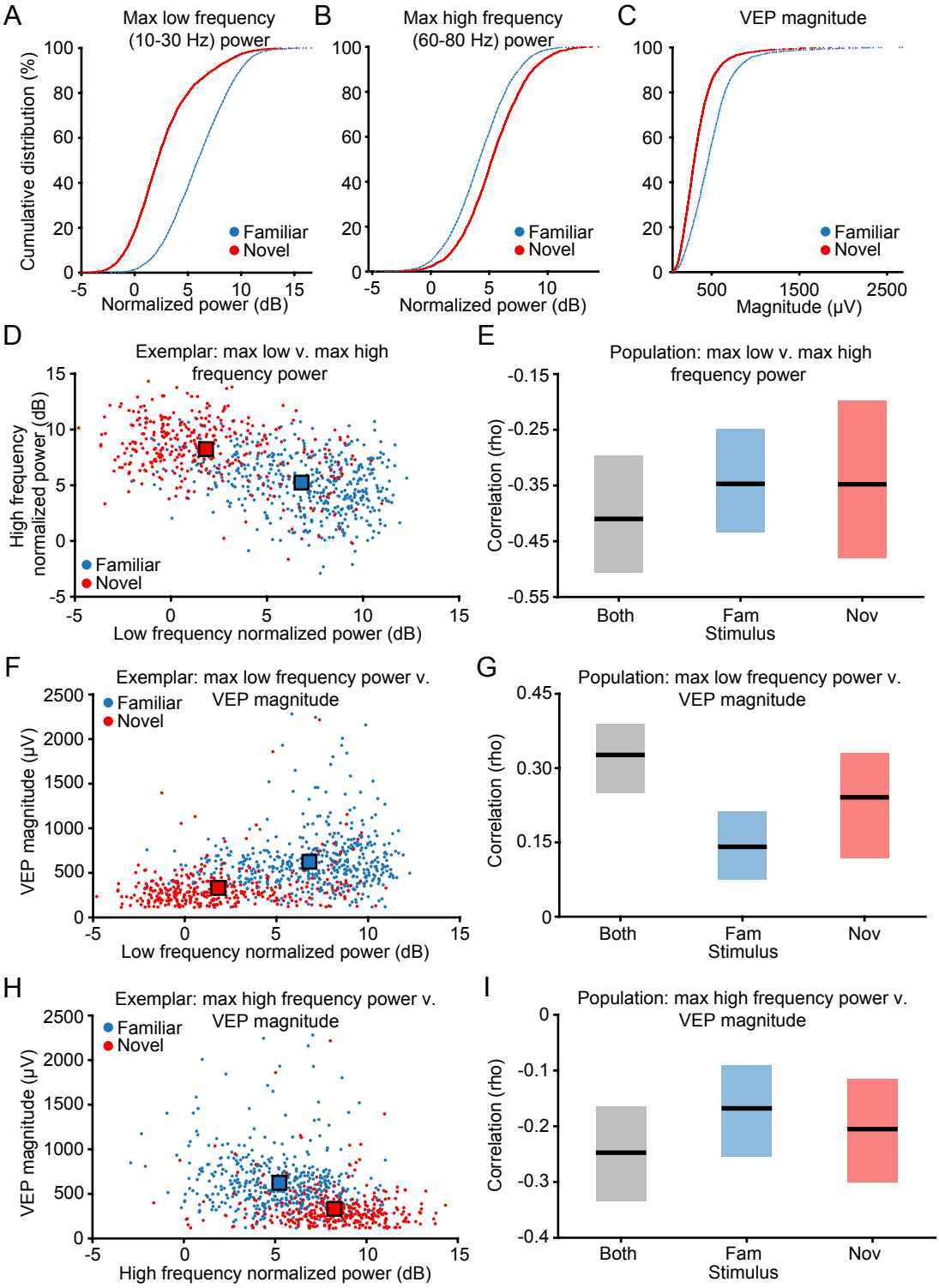
A
Max low frequency (10-30 Hz) power
Cumulative distribution (%)
Normalized power (dB)
Familiar
Novel
B
Max high frequency (60-80 Hz) power
Normalized power (dB)
Familiar
Novel
C
VEP magnitude
Magnitude (μV)
Familiar
Novel
D
Exemplar: max low v. max high frequency power
High frequency normalized power (dB)
Low frequency normalized power (dB)
Familiar
Novel
E
Population: max low v. max high frequency power
Correlation (rho)
Both
Fam
Nov
Stimulus
F
Exemplar: max low frequency power v. VEP magnitude
Familiar
Novel
VEP magnitude (μV)
Low frequency normalized power (dB)
G
Population: max low frequency power v. VEP magnitude
Correlation (rho)
Both
Fam
Nov
Stimulus
H
Exemplar: max high frequency power v. VEP magnitude
Familiar
Novel
VEP magnitude (μV)
High frequency normalized power (dB)
I
Population: max high frequency power v. VEP magnitude
Correlation (rho)
Both
Fam
Nov
Stimulus

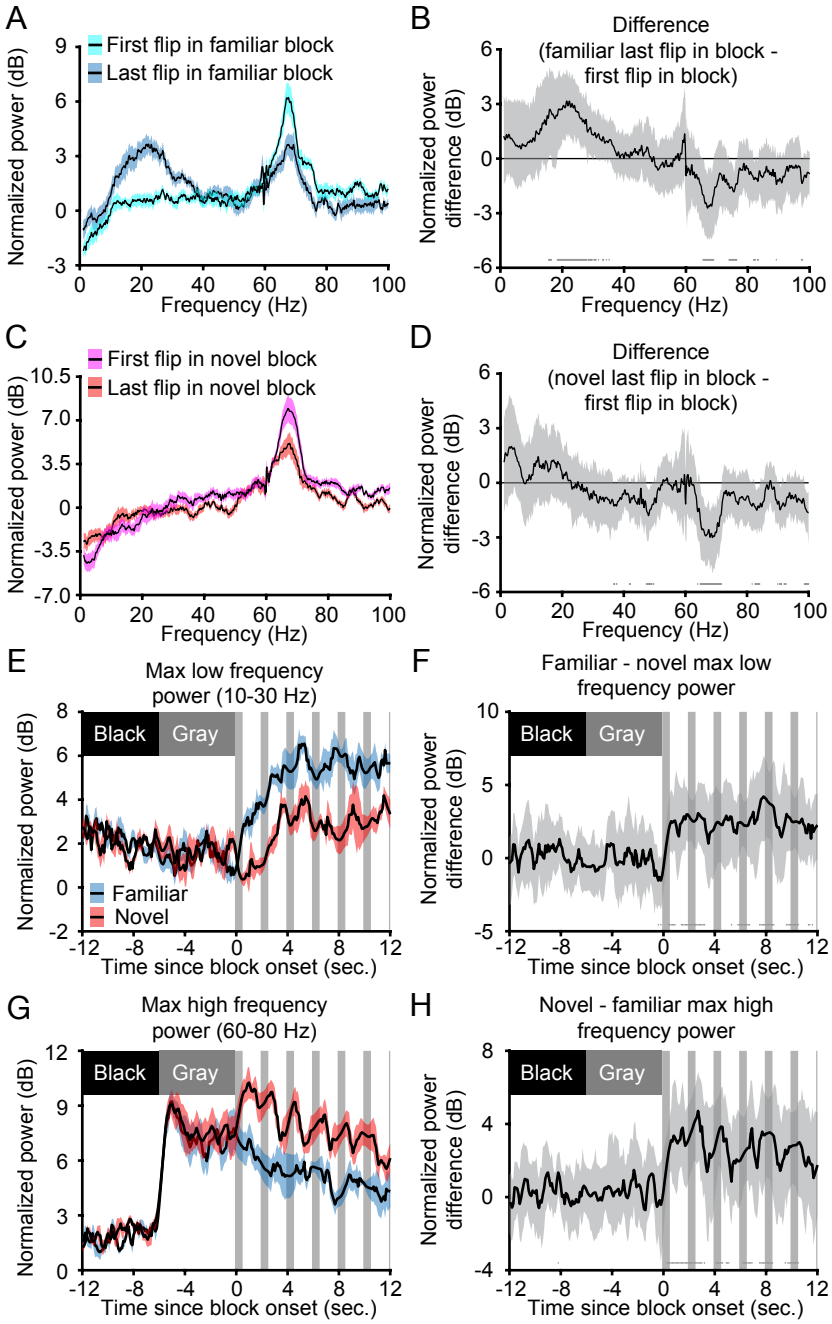
A
First flip in familiar block
Last flip in familiar block
Normalized power (dB)
Frequency (Hz)
B
Difference
(familiar last flip in block -
first flip in block)
Normalized power difference (dB)
Frequency (Hz)
C
First flip in novel block
Last flip in novel block
Normalized power (dB)
Frequency (Hz)
D
Difference
(novel last flip in block -
first flip in block)
Normalized power difference (dB)
Frequency (Hz)
E
Max low frequency
power (10-30 Hz)
Black
Gray
Familiar
Novel
Normalized power (dB)
Time since block onset (sec.)
F
Familiar - novel max low
frequency power
Black
Gray
Normalized power difference (dB)
Time since block onset (sec.)
G
Max high frequency
power (60-80 Hz)
Black
Gray
Normalized power (dB)
Time since block onset (sec.)
H
Novel - familiar max high
frequency power
Black
Gray
Normalized power difference (dB)
Time since block onset (sec.)

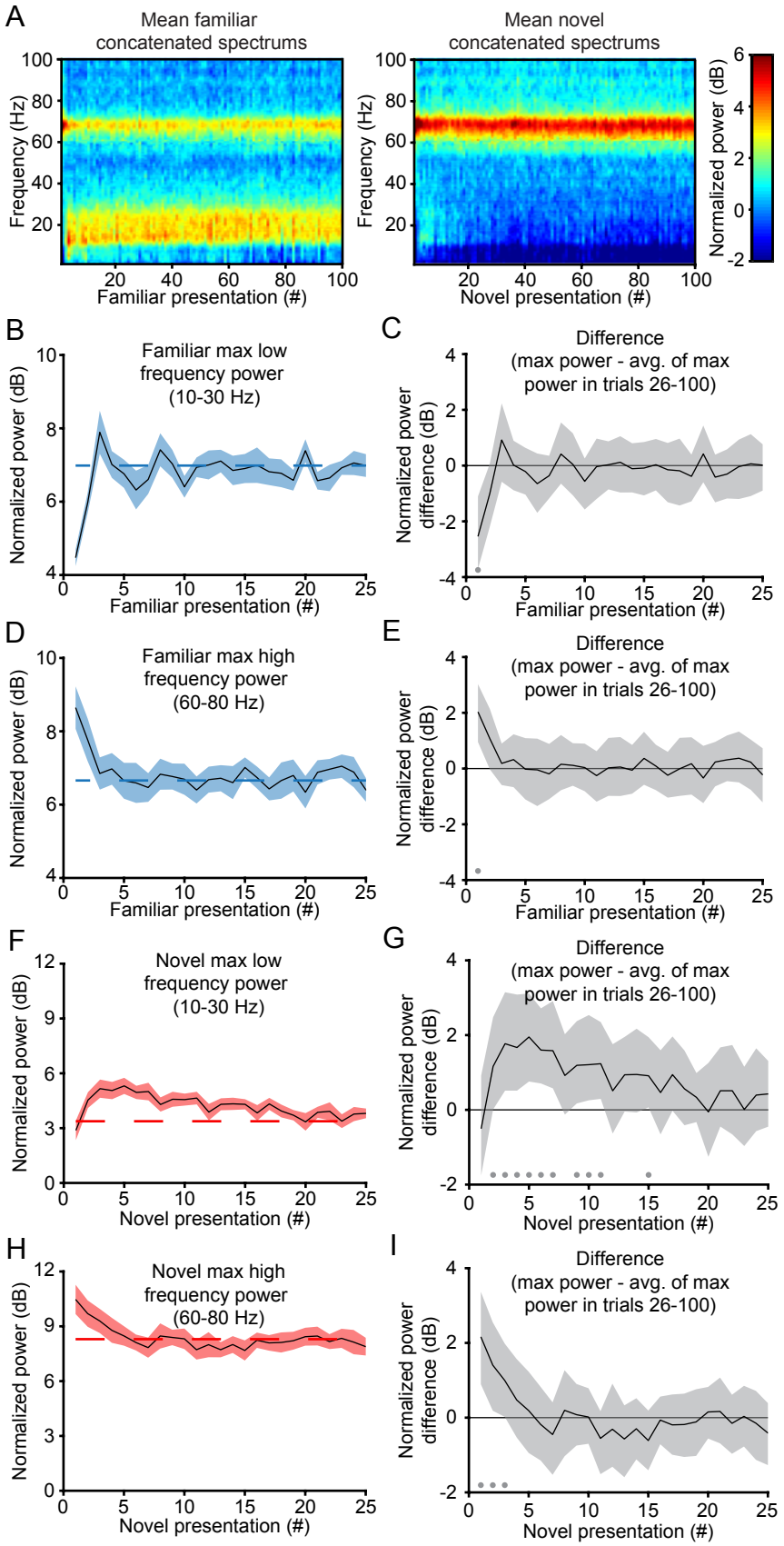
A
Mean familiar concatenated spectrums
Mean novel concatenated spectrums
Frequency (Hz)
Familiar presentation (#)
Novel presentation (#)
Normalized power (dB)
B
Familiar max low frequency power (10-30 Hz)
C
Difference (max power - avg. of max power in trials 26-100)
D
Familiar max high frequency power (60-80 Hz)
E
F
Novel max low frequency power (10-30 Hz)
G
H
Novel max high frequency power (60-80 Hz)
I
Normalized power difference (dB)

Figure 8

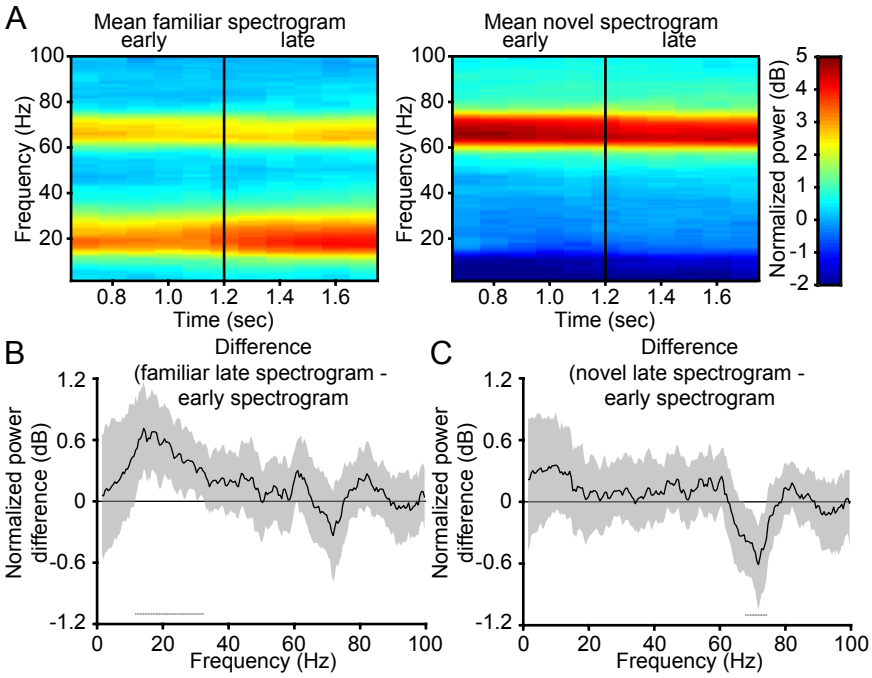
A
Mean familiar spectrogram
early
late
Frequency (Hz)
Time (sec)
Mean novel spectrogram
early
late
Frequency (Hz)
Time (sec)
Normalized power (dB)
B
Difference
(familiar late spectrogram -
early spectrogram
Normalized power
difference (dB)
Frequency (Hz)
C
Difference
(novel late spectrogram -
early spectrogram
Normalized power
difference (dB)
Frequency (Hz)

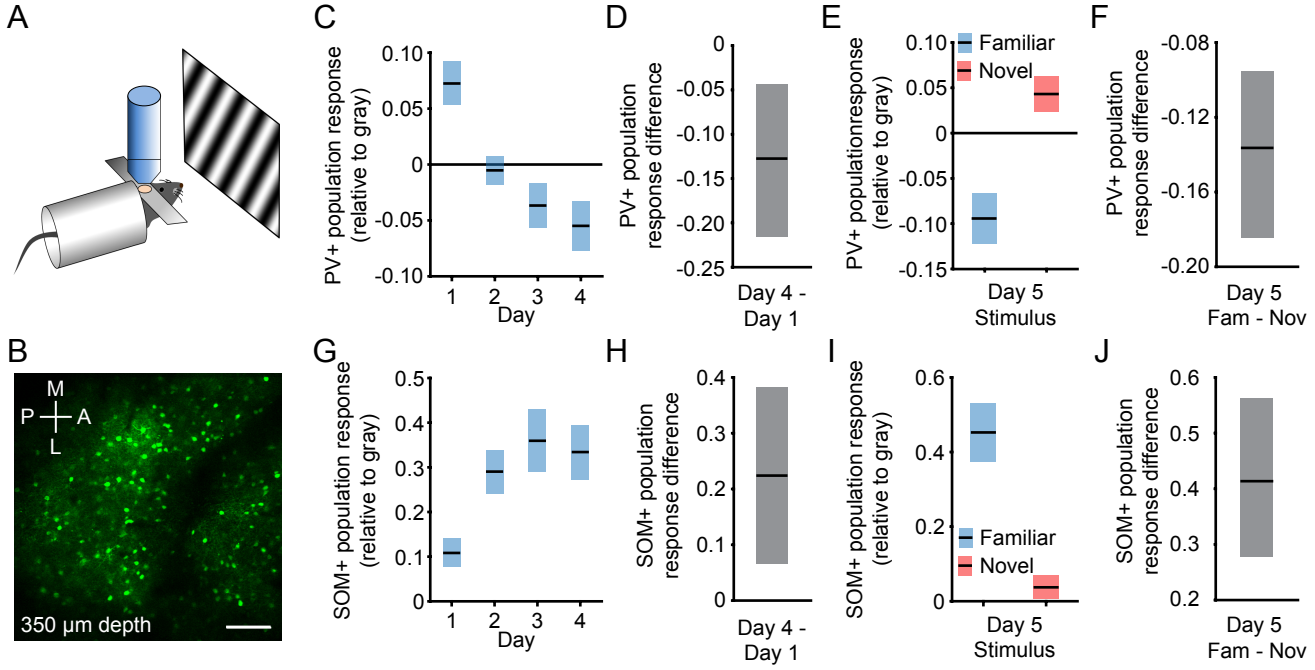
A
B
M
P
A
L
350 µm depth
C
PV+ population response (relative to gray)
0.10
0.05
0
-0.05
-0.10
1
2
3
4
Day
D
PV+ population response difference
0
-0.05
-0.10
-0.15
-0.20
-0.25
Day 4 - Day 1
E
PV+ populationresponse (relative to gray)
Familiar
Novel
0.10
0.05
0
-0.05
-0.10
-0.15
Day 5 Stimulus
F
PV+ population response difference
-0.08
-0.12
-0.16
-0.20
Day 5 Fam - Nov
G
SOM+ population response (relative to gray)
0.5
0.4
0.3
0.2
0.1
0
1
2
3
4
Day
H
SOM+ population response difference
0.4
0.3
0.2
0.1
0
Day 4 - Day 1
I
SOM+ population response (relative to gray)
0.6
0.4
0.2
0
Familiar
Novel
Day 5 Stimulus
J
SOM+ population response difference
0.6
0.5
0.4
0.3
0.2
Day 5 Fam - Nov

Figure 10

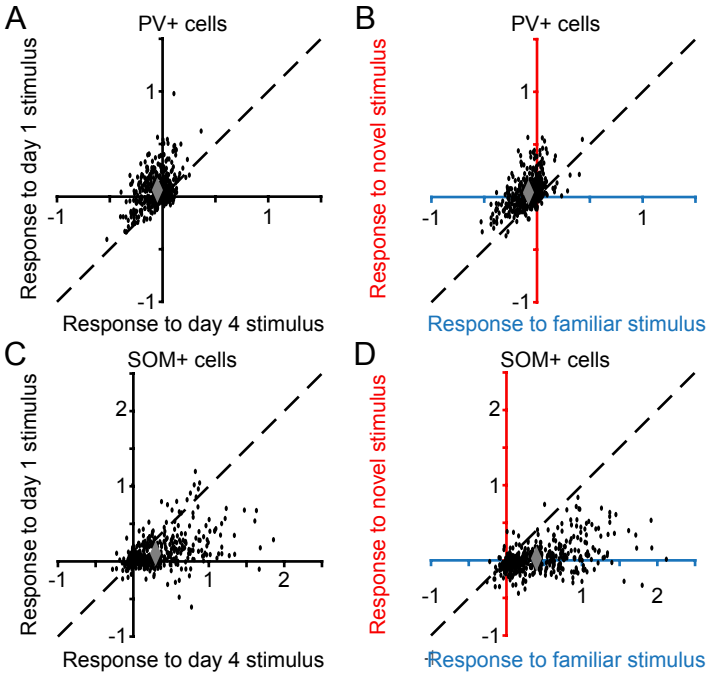
A
PV+ cells
Response to day 1 stimulus
Response to day 4 stimulus
1
-1
1
-1
B
PV+ cells
Response to novel stimulus
Response to familiar stimulus
1
-1
1
-1
C
SOM+ cells
Response to day 1 stimulus
Response to day 4 stimulus
2
1
-1
1
2
-1
D
SOM+ cells
Response to novel stimulus
Response to familiar stimulus
2
1
-1
1
2
-1

Figure 11

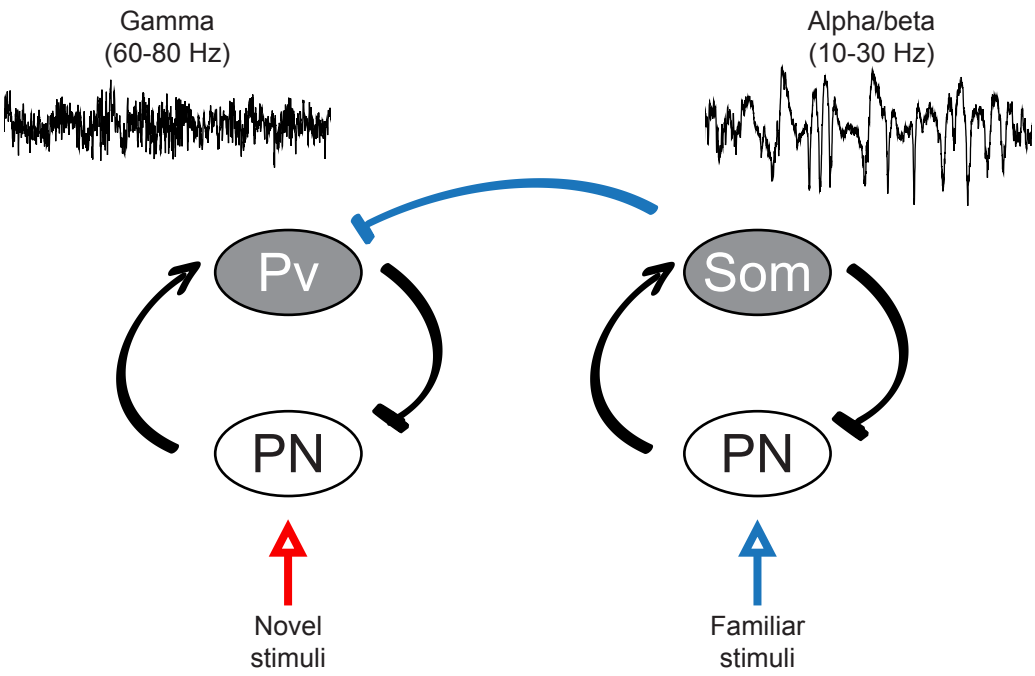
Gamma
(60-80 Hz)
Alpha/beta
(10-30 Hz)
Pv
Som
PN
PN
Novel
stimuli
Familiar
stimuli

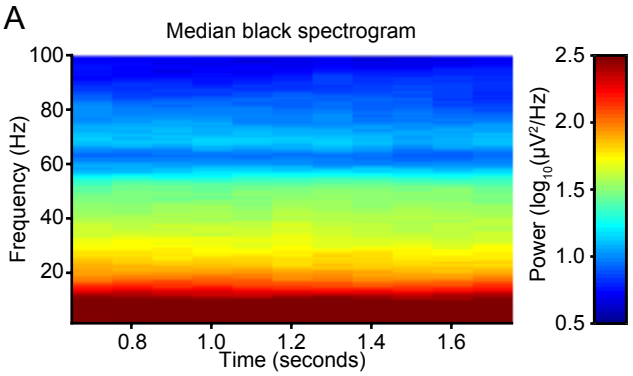
A
Median black spectrogram
Frequency (Hz)
100
80
60
40
20
0.8
1.0
1.2
1.4
1.6
Time (seconds)
Power (log10(μV²/Hz)
2.5
2.0
1.5
1.0
0.5
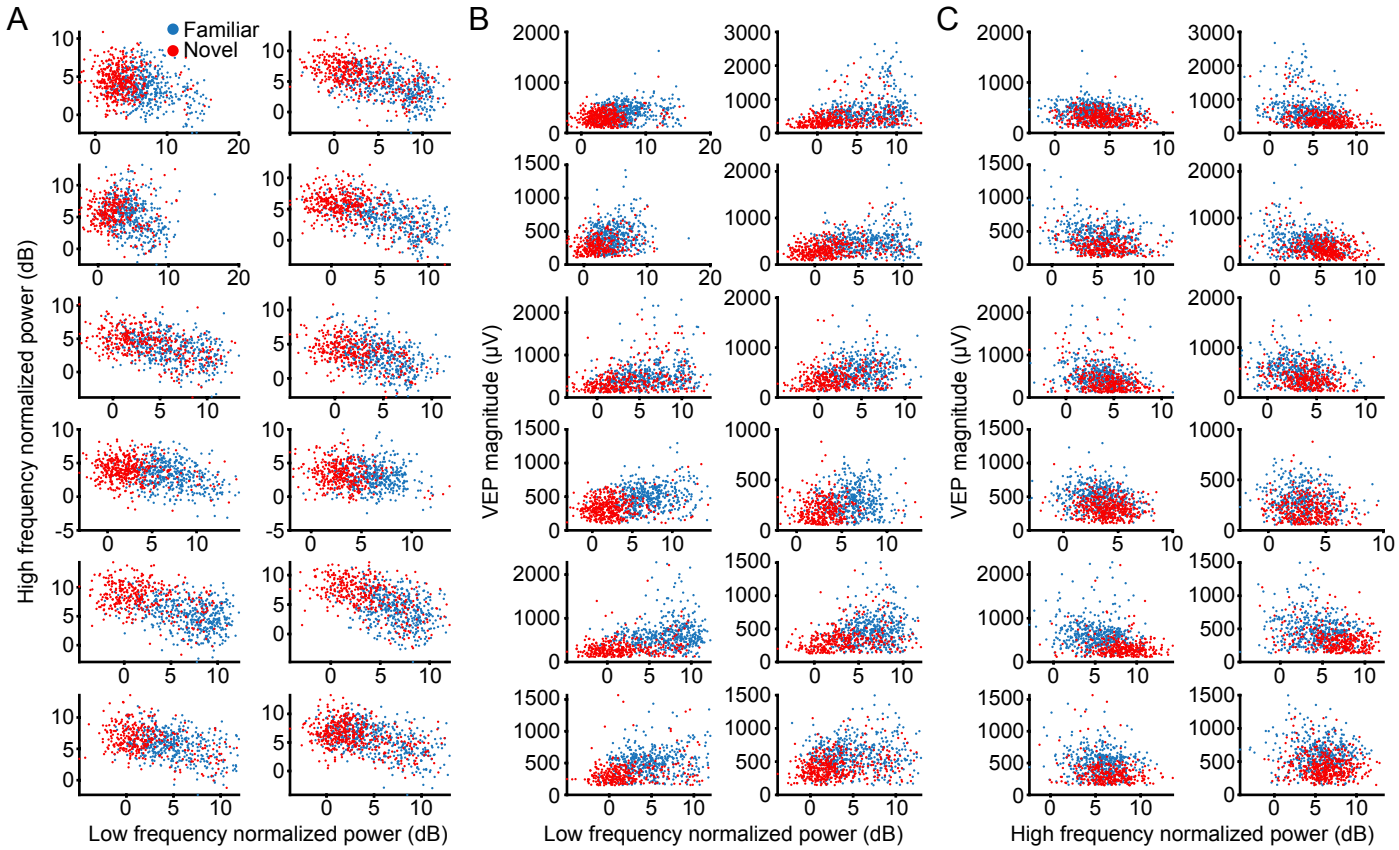
Supplementary Figure 2